UCLouvain

epl

École polytechnique de Louvain

Modeling active distribution grids in power systems voltage stability studies

Author: **Carlos VIDALES FERRO**
Supervisor: **Emmanuel DE JAEGER**
Readers: **Bruno DEHEZ, Caroline LEROI**
Academic year 2019–2021
Master [120] in Electrical Engineering

Acknowledgement

This master's thesis would not have been possible without the support of my parents, my sisters and my wife, who helped and encouraged me to continue working and to overcome the difficulties during this process.

I would like to thank Professor Emmanuel De Jaeger, who continuously guided me, his support was crucial. Not only as a professor, but also as a thesis supervisor, his contributions were essential in the development of the project.

Abstract

The stability of a system is the capacity of the grid to maintain acceptable operating levels when it has been submitted to perturbations. When performing stability studies for the electrical network in computer tools, the loads are normally considered as static loads. This is useful for power flows studies, cable sizing (ampacity analysis), voltage regulation (voltage drop), power system expansion planning, among others. The proposal for this work consists of the modelling of the loads for power system dynamics studies.

There are already several load models that tend to resemble the behavior of the electrical loads under real conditions. Part of this work is to raise awareness of the importance of using a more adequate model when performing stability studies. It should also be noted that the composition of electrical loads has changed significantly over the last 20 years. This means that there are new components involved, among them a lot of power electronics is associated, especially with the rapid growth of electric vehicle chargers and also the large number of distributed generation (residential solar panels) and these have a special impact on the system stability results. And to be more precise according to the scope of this work, they have a significant impact on voltage stability.

Glossary

CIGRE	International Council on Large Electric Systems
CMPLD	Composite Load Model
CPF	Continuous Power Flow
DG	Distributed Generation
DSO	Distribution System Operator
ELIA	Belgian Transmission System Operator
IEEE	Institute of Electrical and Electronics Engineers
IES	International Energy Agency
NERC	North American Electric Reliability Corporation
OLTC	On-load tap-changer
PSAT	Power System Analysis Toolbox for MATLAB
RES	Renewable Energy Sources
SNB	Saddle-Node Bifurcation
TSO	Transmission System Operator
WECC	Western Electricity Coordinating Council
WSCC	Western System Coordinating Council

NOTE The abbreviation “P-V” is used for "Active Power - Voltage" representation, and the abbreviation "PV" is for “Photovoltaic”.

Contents

Introduction

The electricity, nowadays, is a vital part for our modern comforts. But also, generally speaking, it stimulates the economy by optimizing the productivity, and it is important for medical cares and treatments.

Therefore, the need for this to reach everywhere in good conditions is a complex and important role. This is done by the Transmission System Operator (TSO) and the Distribution System Operator (DSO). Any important change to the system (new load, new line, system expansion, among others) should be informed and developed together with the System Operator (SO), so that the necessary operational maneuvers and studies can be carried out to ensure the correct functioning of the system.

Also considering operations, perturbations, faults, among others, the SO needs to be aware of the real equivalent circuit model of the system. At this point a question could be raised, how were the electrical elements affected? (For example, a parallel line disconnection will change the equivalent representation electrical circuit of the global transmission line).

For the purpose of this project, the effect of these changes on the voltage stability of a system, will be analyzed. Some question that will be addressed are: is it important to perform voltage stability studies when doing planning studies? How important is it to know at what operating point the system is working? How much can the response of the electrical system be affected by not having realistic models (that resemble real behavior according to the different elements that can be found in the network)?

To address these questions, the master's thesis is developed following this structure:

1. Chapter 1 gives the description of the problem and the general behavior of the system considering the load characteristic and some perturbations that could happen.

2. Chapter 2 introduces some of the different electrical loads that can be found in the grid with their respective theoretical representations.

3. Chapter 3 discusses the different approaches that can be used to estimate a model for an existing network distribution.

4. Chapter 4 describes the methodology used on this work to estimate the electrical model for an approximate consideration of a small Belgian power system.

5. Chapter 5 studies the effect on voltage stability of using the model developed.

Chapter 1

General Description

In order to understand the purpose of this project, this chapter will describe the general environment of an electrical network and the problems that can occur regarding the stability of the system. Also, a basic explanation of the point of operation in the grid will be addressed.

1.1 Context

There are several factors within an electric grid that can lead to a blackout, these conditions affect the stability making the system to collapse. some of these conditions can be overload of electrical lines/transformers/etc., system faults (components failure, short circuits), wrong maneuvers (human mistake, control/protection system mistake), and others. These conditions directly affect the grid stability and may lead to a complete power outage. Some of the most known are the ones that took place in Tokyo in 1987, in the United States in 2003 and in Europe in 2006 [1][2].

In Belgium, the TSO is ELIA which has a crucial job on transmitting electricity all over the country. The voltages used for transmission goes from 30 kV up to 400 kV, with a frequency of 50Hz. The TSO is in charge of maintaining a reliable, sustainable, and affordable grid. To create a complete reliable system, the TSO, and the DSO (in charge on the low voltage distribution) must work together. There must be constant communication between them for the protection mechanisms to work properly.

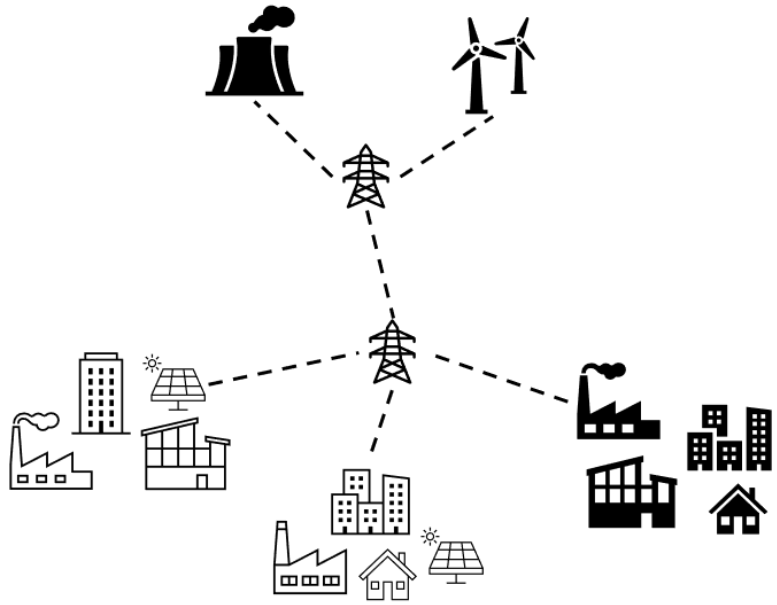

Figure 1.1: General power distribution system

Indeed, there are protection systems that try to isolate the faults as fast as possible but of course there can exist cases were the system is already in an instability point and the possible actions to be made does not have positive expected results. Also, the N-1 contingency is not always fulfilled. Nowadays, most of system have back up equipment, secondary lines, by-pass systems, among others, to ensure that local faults are cleared and separated to maintain or reestablish the system operation.

The correct way to start analyzing this problem is by first starting to classify the power system stability. The electrical grid is considered to be stable if after a perturbation it can: maintain synchronism through torque balance of synchronous machines (Rotor angle stability), maintain the frequency values within acceptable ranges through demanded and generated power balance (frequency stability), and maintain the voltage levels in acceptable values through reactive power balance (voltage stability) [3].

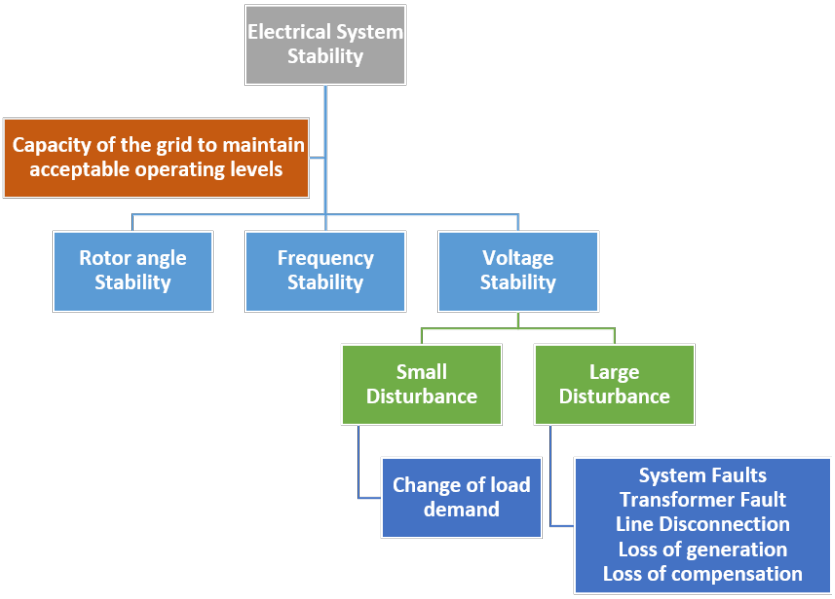

Figure 1.2: System Stability Classification

For this project only the voltage stability analysis will be taken into account. It can be classified as well from the severity of the perturbation. The small disturbance is mainly given from the variation of the load (increase/decrease) and the large disturbances are given from system faults produced from components failures, short circuits (internal or external factors), wrong operations, and others.

1.2 Voltage Stability

When creating or analyzing an electric power system, voltage stability is one of the major concerns. Voltage stability is defined as the capacity of the system to maintain an acceptable voltage profile after having been exposed to a disturbance.

A way to determine the instability is by considering a simple power system (see **figure 1.3**), consisting in a single transmission system with a single source, an equivalent feeding impedance (that includes the transmission lines and the transformer equivalent circuit), and an equivalent impedance for the load side.

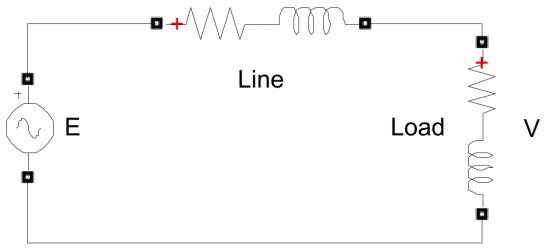

Figure 1.3: Oneline simple transmission circuit

Understanding how power flows through a transmission system is the best way to comprehend the fundamentals of voltage stability. There is a sending end with the source (generator) and a receiving end where the load is connected. A radial complex power flow is represented in figure[1.4].

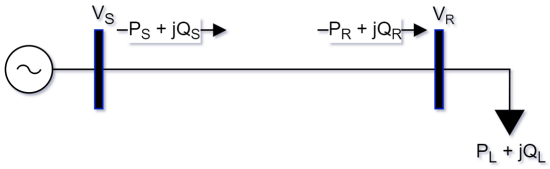

Figure 1.4: Complex power transmitted

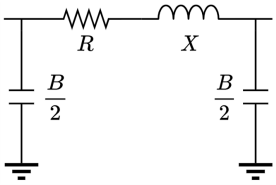

Figure 1.5: Line π model

The complex power flow is governed by the power factor angle δ. Also, for a simple analysis, a short length line is used (this means that the resistance R of the transmission line will be neglected).

$$\begin{aligned} P_S = P_R = P_L &= \frac{|V_S||V_R|sin(\delta)}{X} \\ Q_R = Q_L &= -\frac{|V_R|^2}{X} + \frac{|V_R||V_S|cos(\delta)}{X} \\ Q_S &= \frac{|V_S|^2}{X} - \frac{|V_R||V_S|cos(\delta)}{X} \end{aligned} \tag{1.1}$$

From re-arranging the complex power flow expressions [4], and solving for the voltage at the receiving end V_R, it is possible to obtain:

$$|V_R|^2 = \frac{|V_S|^2}{2} - P_L X tan(\delta) \pm \sqrt{\frac{|V_S|^4}{4} - P_L X(P_L X + |V_S|^2 tan(\delta))} \tag{1.2}$$

To be able to obtain the Active Power vs. Voltage curve at the receiving bus (V_R), the load at the receiving end will vary by increasing in small steps ($\Delta P << P_{nominal}$). It means that the impedance of the load at every step it will decrease. This will be done for a specific power factor in the load and for a fix voltage in the sending end. In **figure 1.6** different P-V curves are obtained, each one is using a specific power factor for the load at the receiving end. The feeding line used has a reactance (X) of 0.5 pu, and the voltage at the sending end (V_S) is $1\angle 0°$ pu.

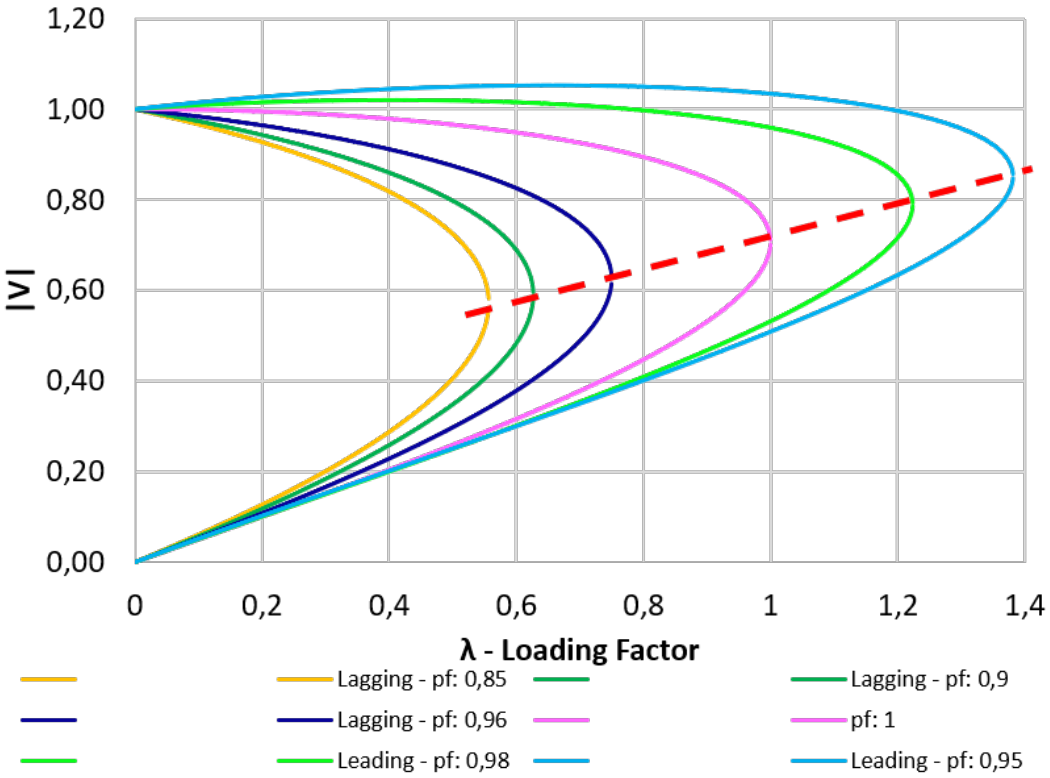

Figure 1.6: P-V curve analysis

This is one of the methods for studying the voltage stability problem, known as the **P-V curve** method. The nose point of this curve represents the stability limit, indicating that the operation above this point is in the stable region, and below is in the unstable region.

Another well-known criteria for determining the instability, is when the bus voltage (at least in one bus on the grid) decreases as the reactive power injection is

increasing for the same bus[4]. This corresponds to the Voltage-Reactive Power (V-Q) sensitivity, stable for a positive sensitivity and unstable for a negative sensitivity. This is important to consider given the fact that nowadays shunt compensations are extensively used.

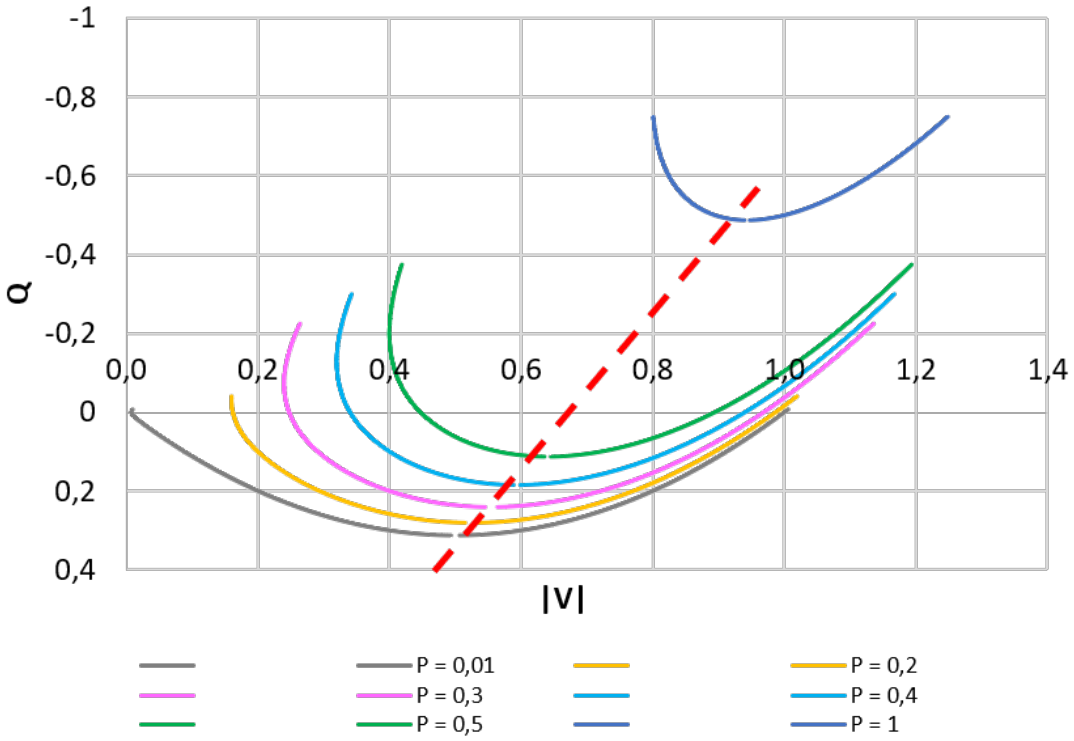

Figure 1.7: V-Q curve analysis

To be able to obtain the Voltage vs. Reactive Power curve at the receiving bus (V_R), the reactive power injection at the receiving end will vary by increasing in small steps ($\Delta Q_{compensation}$). This will be done for a specific power factor, a fix voltage in the sending end, and at constant load. The **equation 1.2** is used as well for this method. For this representation, the feeding line used has a reactance (X) of 0.8 pu, the voltage at the sending end (V_S) is $1\angle 0°$ pu, and the power factor of the load is 0.8 (lagging). Each color curve shown in **figure 1.7**, is obtained from different fixed loads in the receiving end (P_{load} =0.01, 0.2, 0.3, 0.4, 0.5, or 1).

This method is known as the **V-Q curve** method. The knee point of this curve represents the stability limit, indicating that the operation in the right of this point is in the stable region (positive dq/dv slope), and in the left is in the unstable

region.

1.2.1 Software used for analysis

The computer software that was used for modeling and analysis was the Power System Analysis Toolbox (PSAT [5]). This is a free no-warranty toolbox developed for MATLAB with a general public license for educational or private purposes. This software was chosen because it allows to perform power flow analysis, and voltage stability analysis using the P-V curve method called the Continuation Power Flow (CPF).

Power flow [5]

On this method the power flow and the voltage profile at each bus is calculated. The general methodology is:

1. Initialize the system algebraic variables.
2. Solve with Newton–Raphson iteration method.
3. Determine the voltage magnitude and angle on the buses of the system that satisfies power balance.

Continuous power flow methodology [5]

On this method the P-V curve method for the voltage stability analysis is computed. The general methodology is:

1. Predictor step realized by the computation of the tangent vector at each step.
2. Corrector step obtained by the local parameterization or a perpendicular intersection.
3. Compute the value of the loading parameter (λ) for the Saddle-Node Bifurcation (SNB) point.

1.3 Power system general behavior

For this section, the concept of the operating point for different loads will be addressed.

Voltage dependent load

It must now be considered that electrical loads can have different characteristics. For instance, there can exist voltage dependent loads (additional explanation will be done in **section 2.2.1**) in which the power demanded is linked to the voltage exposed.

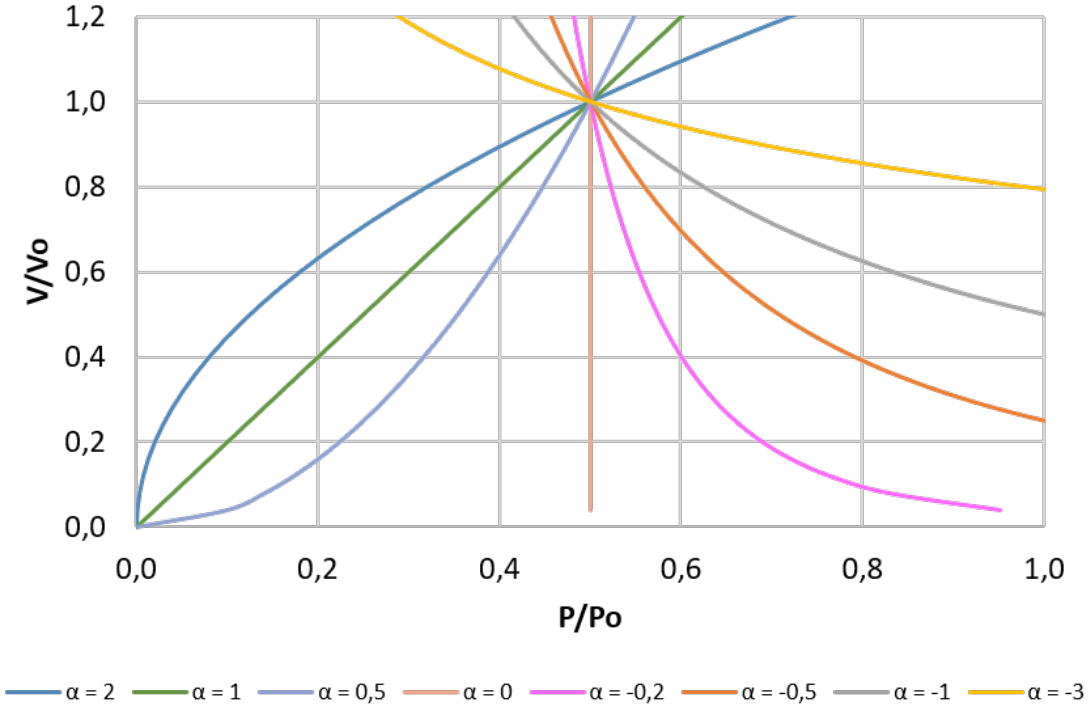

Figure 1.8: Load Characteristic

For example, a voltage dependent load with a constant impedance behavior ($\alpha = 2$) will have an approximate operating in the intersection with the system P-V curve (see intersection point on **figure 1.9**). If the intersection is above the critical point (nose point), the system is considered to be operating in the stable region. If it happens that there is no apparent intersection point, it could be considered to be in an unstable condition.

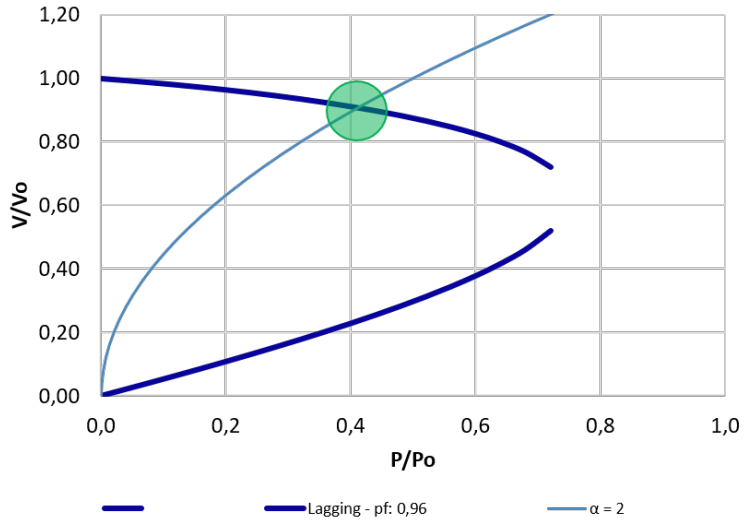

Figure 1.9: Load - Estimated operating zone

When a fault occurs in the system, some elements can be disconnected (for example a line loss) to isolate the fault leading to a new configuration of the system. This new arrangement of elements affects the equivalent impedance of the feeding line to the load (or the bus analyzed), meaning that the P-V curve of the system at a specific bus change.

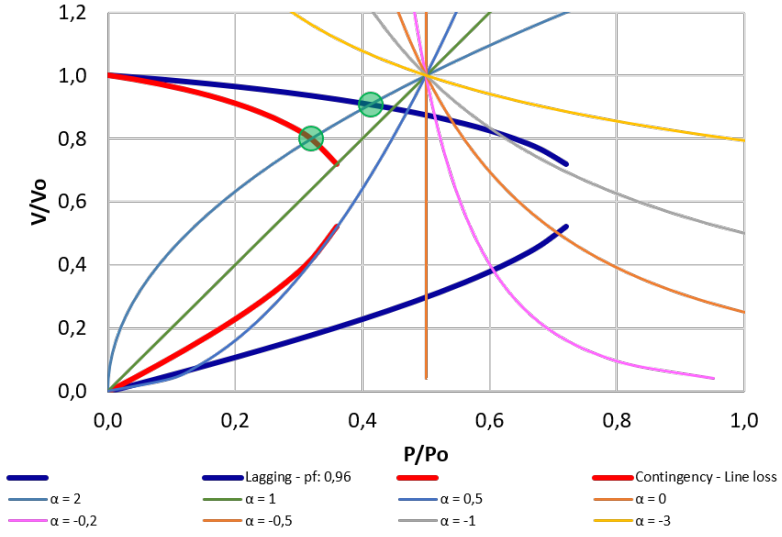

Figure 1.10: Load - Estimated operating zone when line loss

This new curve will represent a new operating point for the load (e.g., constant impedance $\alpha = 2$). The electrical system will enter into an unstable condition if the curves does not intersect (load characteristic curve and P-V system curve).

To summarize this chapter, there is a need to perform voltage stability analysis in a system. The voltage conditions in the network can drastically change due to maneuvers, operations or faults, and these can even lead to total collapse.

Chapter 2

State of the Art

In this chapter the general composition and characterization of the electrical loads, are addressed. Also, the electrical models and their equivalent circuit representations are described.

2.1 Electrical Load Characterization

There are different ways to characterize an electrical load in an electrical grid. Normally when talking about a load they can be classified by nature as resistive, inductive and/or capacitive. When discussing how they are distributed in the system, they are spread mainly in 4 different sectors (residential, industrial, commercial, Agriculture, others). But as well, each one of those could be divided by class (heating devices, induction motors, electronic equipment, others).

To have a more realistic behavior, it must be established that loads are not constant, there are several factors which determine the consumption in time domain, and they can be characterized by the time of the day, the day of the month, the season and also the weather, among other factors.

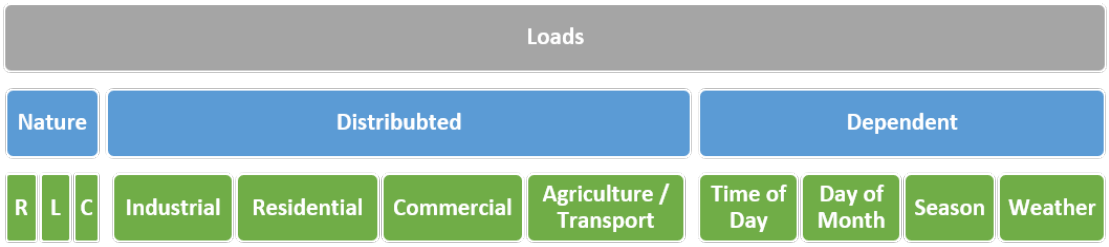

Figure 2.1: Electrical Load Characterization

A specific electrical load can also have different operating parameters such as load factor, demand factor and diversity factor. These will help mainly to do market analysis or planning studies.

Having a detailed model considering every single parameter and also considering every component/load demand is not possible. There are computational limitations for all the amounts of buses/variables that will be needed. And also, the complexity of the calculations for the different types of analysis will make the system extremely difficult to converge. This will also impact the analysis time.

Then to overcome this problem in a power system analysis, to be able to quantify and characterize the composition of the load easier, a grouping/aggregation of the loads on the main buses must be done.

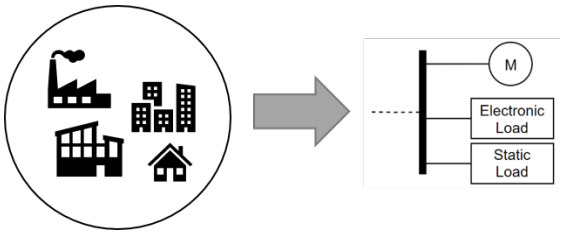

Figure 2.2: Electrical load equivalent

A building, a neighborhood, an area, a town, or even a city, can be represented with a simpler and general equivalent model. But now the drawback is that this model must represent as close as possible the grid dynamics. Therefore a correct aggregation of the loads must be done, not only considering active and reactive powers of each load but taking into account the different parameters depending on the specific load model. [6]

Finally, due to the increasing PV panel use in the Belgium grid, this component will be considered. To have a rough quantification of the amount of panels (power) to use, there is a proposal that has as a goal to supply 40% of electricity from renewable sources by 2030 and 100% by 2050 [7]. This is designed to gradually left a side the highly use of nuclear sources nowadays. For the scope of this project, the system element that will be used in the model will be only the approximate representation of residential solar panels in Belgium's houses.

2.2 Load Models

This section will be addressed to cover the general concept of the different load models used to develop the model.

2.2.1 Exponential Load

This model, also known as a voltage dependent load model, has 2 exponents variables that represent the sensitivity factors of the powers with respect to the voltage.

$$\begin{aligned} P_{exp} &= P_n \left(\frac{V}{V_n}\right)^{\alpha_P} \\ Q_{exp} &= Q_n \left(\frac{V}{V_n}\right)^{\alpha_Q} \end{aligned} \tag{2.1}$$

This type of model is used to represent mainly single constant current, constant power, or constant impedance loads, but as it will be seen in the next model, many loads are composed with the mixture of these and even others. The impact of the different exponents α can be seen in figure [1.8].

2.2.2 Polynomial Load

Also known as the ZIP model, this model is represented by a constant impedance load model, a constant current load model and a constant power load model. These is obtained by applying respectively 2,1,0 as the exponents on the exponential load model seen before.

$$\begin{aligned} P_{zip} &= P_n \left[p_z \left(\frac{V}{V_n}\right)^2 + p_i \left(\frac{V}{V_n}\right) + p_p\right] \\ Q_{zip} &= Q_n \left[q_z \left(\frac{V}{V_n}\right)^2 + q_i \left(\frac{V}{V_n}\right) + q_p\right] \end{aligned} \tag{2.2}$$

The z, i and p coefficients represent in p.u. the contribution of each type of load, constrained to complete 1 p.u. (100%).

2.2.3 Polynomial Load - Electric Vehicle

The electric vehicle charger consists of a bridge rectifier (single phase or three phase), which is the AC-to-DC conversion stage, followed by a typical buck converter, which

is the DC-to-DC conversion stage, where the batteries of the plug-in electric are being charged.

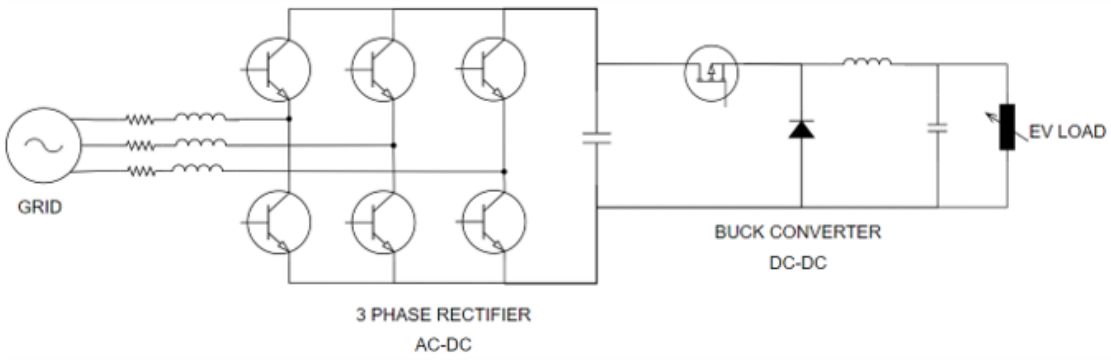

Figure 2.3: EV charger scheme [8] [9]

Following an analytical analysis, a detailed representation of the charger is done in [8][9]. In general, with the equations of the circuit analysis of the buck converter and by adding the additional stages (input filter, active rectifying, and the battery equivalent) with their circuit model expressions, the relationship of the load demand (P) with respect to the voltage (V) is found. The practical representation for the relationship of this system is described in **equation 2.3**.

$$\begin{aligned} \frac{P}{P_0} &= a \cdot \left(\frac{V}{V_0}\right)^{\alpha} + b \\ \frac{Q}{Q_0} &= \frac{S}{S_0} \cdot sin(\theta) \\ \frac{S}{S_0} &= \frac{\frac{P}{P_0}}{cos(\theta)} \end{aligned} \tag{2.3}$$

Where **b** will represent the fraction of constant power and **a** will represent the fraction of the exponential load type (voltage dependent, as seen in **equation 2.1**) but with a negative exponent α. There are several elements that have an important influence on the negative factor (α), such as the parasitic resistance of the input filter, the turn-on resistance of the semiconductors, and also the resistance in the feeding conductor. After solving for the different elements that could be present in the electric charging chain, the parameters used to represent and characterize the behavior of the EV system are displayed in **table 2.1**.

a	0.07
b	0.93
α	-3

Table 2.1: EV characterization Parameters

2.2.4 Induction Machine

For the electrical circuit of the induction motor, the third order model representation is used [10] [11]. Working with the same principle as a transformer, the current in the stator winding creates a magnetic field producing an electromagnetic induction, which induces a voltage on the rotor. An equivalent representation for a steady state of the motor is shown in **figure 2.4**.

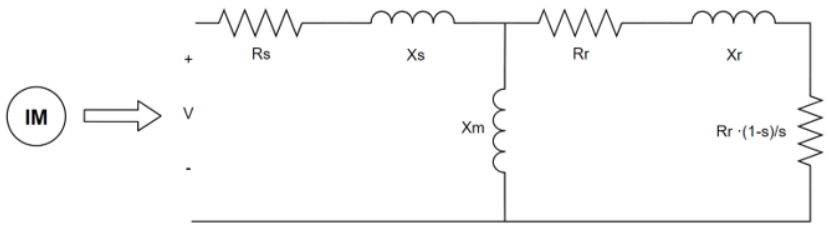

Figure 2.4: IM Electrical Circuit

The Rs and the Xs represents the impedance of the stator winding, the magnetizing reactance is Xm and, Rr and Xr represents the rotor impedance. After simplifications, the equivalent impedance for the IM is obtained in **equation 2.4**.

$$\begin{aligned} Z_{IM} &= R_{IM} + jX_{IM} \\ R_{IM} &= \frac{X_m^2 R_r s}{R_r^2 + (X_m s + X_r s)^2} + R_s \\ X_{IM} &= \frac{X_m^2 X_r s^2 + X_m X_r^2 s^2 + X_m R_r^2}{R_r^2 + (X_m s + X_r s)^2} + X_s \end{aligned} \tag{2.4}$$

For constant speed operation, the mechanical load that is applied on the rotor will set a slip value on the machine which is used to determine the equivalent impedance. Knowing the slip, the power demanded from the machine can be found (as seen on **figure 2.8** and **2.10**). Also, the power factor can be calculated (see **figure 2.5**).

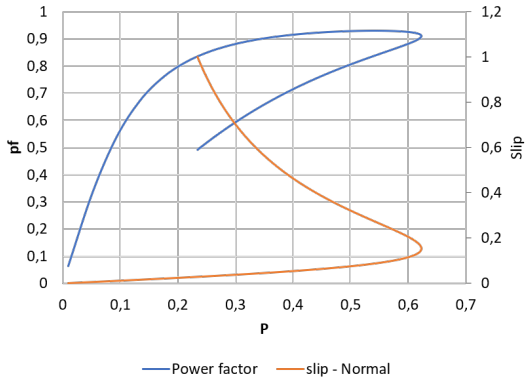

Figure 2.5: IM Slip - power factor relation

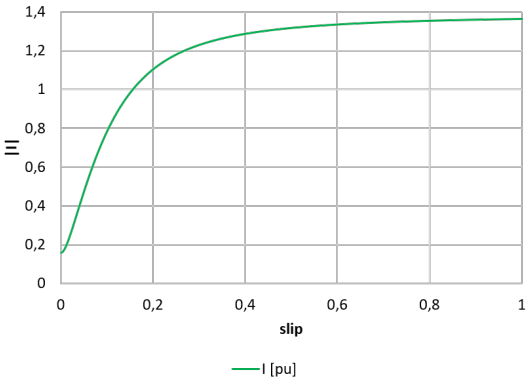

Figure 2.6: IM Slip - current relation

General Behavior

On this part, a general behavior (operating conditions) regarding the system environment is considered. The way how the impedance changes when the load changes has a significant impact in P-V curve in the system. The equivalent impedance of the induction machine is linked to the slip. Starting from the point that the motor is rotating almost at nominal speed ($slip \approx 0$, $speed \approx 1$), when the load at the motor (the resistive torque) starts to increase the slip starts to increase (the speed starts to decrease) until the critical.

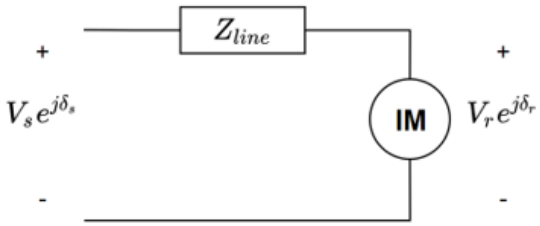

Figure 2.7: IM general circuit

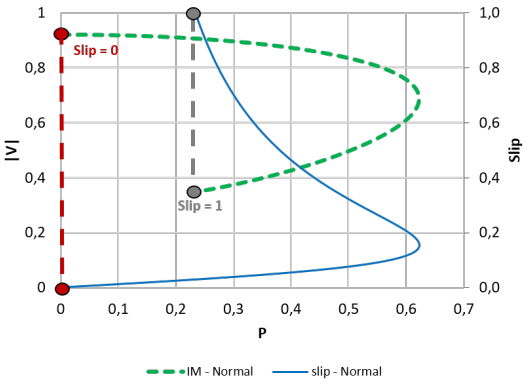

Figure 2.8: IM P-V curve

The P-V curve is obtained from solving the voltage and the power at the receiving end (V_R and P_R) for every possible value of the slip (0 - 1). When the machine has no apparent mechanical load and the rotation is almost at the synchronous speed (s=0), there is still a demand of energy produced by the stator. At the opposite end (s=1), when the rotor is locked and the machine is stalled, the

machine demands a significant amount of energy due to the losses in the active elements (high current demand when the slip increases, as seen in **figure 2.6**). The parameters used for this system representation (Electrical circuit seen in **figure 2.4**) are presented in **table 2.2**.

$$\begin{aligned} V_r &= V_s - Z_{IM} I \\ I &= \frac{V_s}{Z_{line} + Z_{IM}} \\ S_{IM} &= P_{IM} + jQ_{IM} = V_r I^* \end{aligned} \tag{2.5}$$

Parameter	Value	Unit
Rs	0,03	pu
Xs	0,11	pu
Rr	0,10	pu
Xr	0,11	pu
Xm	5,75	pu
Xline	0,5	pu
Vs	1	pu

Table 2.2: IM test parameters

The maximum torque or power that can be transmitted (see **figure 2.10**) to the induction machine before reaching the nose (see **figure 2.8**) is affected as well by the impedance of the line, a smaller impedance represents a bigger power that can be extracted.

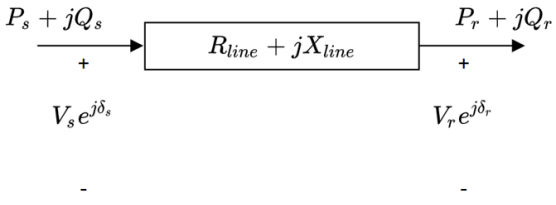

Figure 2.9: Power transfer line

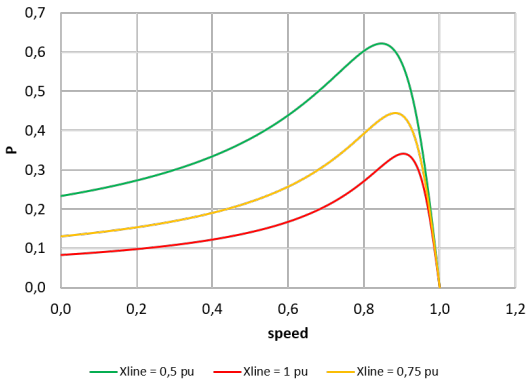

Figure 2.10: IM Power - Speed curve

For this case as well, when a fault occurs in the system some elements can be disconnected (for example a line loss) to isolate the fault leading to a new configuration of the system. This new arrange of elements affect the equivalent impedance of the feeding line to the load affecting the maximum power as well.

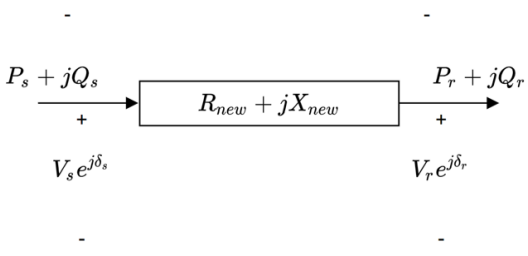

Figure 2.11: Power transfer line loss

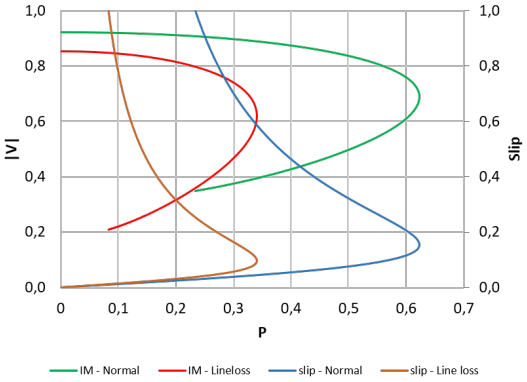

Figure 2.12: IM P-V curve line loss

This means that the P-V curve of the IM system changes. Now the maximum power of the IM is decreased (e.g., the new impedance increased by a factor of 2, then the maximum power decreased by a factor of 2).

To conclude this chapter, with the use of existing models (such as the exponential load type, the polynomial load type and the induction motor type), most of the electrical elements present in the system can be represented. It means that these elements can be put together to represent the equivalent of the various electrical charges of a grid.

Chapter 3

Load Estimation Approach

On this section, the method to estimate the parameters will be addressed. The accuracy of the model will have a significant impact on the power system stability analysis, but to have a more accurate model will also lead to high complexity. Basically there are two approaches [12] [13] to estimate the model parameters. The objective is to aggregate appropriately the different electrical elements from a specific point (e.g., downwards a medium voltage load bus), considering a good generalization capability, it means that the compromise between complexity and error is optimal.

3.1 Measurement Based

This method consists on a mathematical identification problem [12]. There will be needed to expose the system to different perturbations to characterize the system. The disturbances can consist of tap changes, lines disconnections, load disconnections.

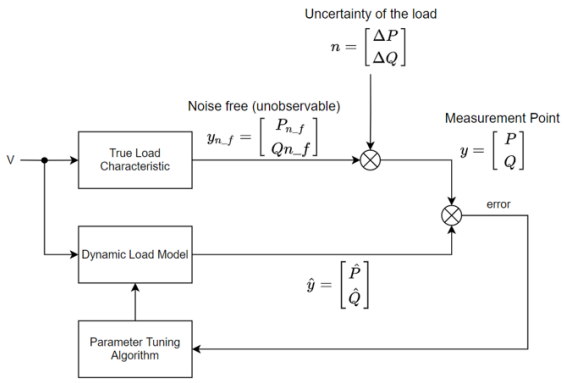

Figure 3.1: Measurement Based Approach Scheme[12]

The drawback is that to expose the system (a big system) to perturbations is not always an easy task, there are big risks on performing these kinds of maneuvers. Also, these disturbances should also be sufficiently noticeable, and preferably over long periods, to capture the nature of the loads. Additional, it is important to remark that for the model to be correctly tuned, a large amount of data will be required.

3.2 Component Based

First, to be able to make a model that contains the different kinds of loads present in the system, it is necessary to understand and to decompose the electricity distribution in the grid. First, a separation by sector (i.e., industrial, residential, etc.) is done, then a class section is imposed (i.e., heating devices, electronic devices, etc.), and finally a classification by type of load is used. For the purposes of this work, the values will be adapted to the Belgium electric system.

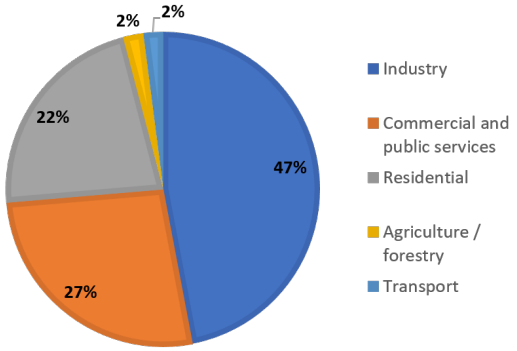

Figure 3.2: Electricity Consumption by Sector - Belgium 2018

These distribution was obtained from the IEA data [14]. The newest report, considering the electricity consumption by sector in Belgium, is from 2018.

3.2.1 Parameters Aggregation

Following the component-based approach, it is necessary to apply a type aggregation on the load to be able to simplify the model, but still try to keep the general behavior of the system. Each load has an active and a reactive power component that can be merged. the active components can be added with their own kind directly due to the energy conservation law. On the other hand, this cannot be

done directly with the reactive power components, they must consider the power factor of each load.

Electronic and Static loads

Due to the many different types of loads assigned to each class, which, at the same time, are also assigned to specific sectors, an aggregation is needed. First a type aggregation is needed as represented in equation [3.1]. Then, a class aggregation is performed as represented in equation [3.2]. Finally, the sector aggregation (equation[3.3]) is done to obtain the equivalent parameters for the ZIP model.

$$\begin{aligned} p_{(z,i,p)_{type-agg}} &= \sum_j \%type_j \cdot p_{j_{(z,i,p)}} \\ q_{(z,i,p)_{type-agg}} &= \frac{1}{Q_{class}} \sum_j \%type_j \cdot q_{j_{(z,i,p)}} \cdot Q_{type_j} \end{aligned} \tag{3.1}$$

$$\begin{aligned} p_{(z,i,p)_{class-agg}} &= \sum_k \%class_k \cdot p_{k_{(z,i,p)_{type-agg}}} \\ q_{(z,i,p)_{class-agg}} &= \frac{1}{Q_{sector}} \sum_k \%class_k \cdot q_{k_{(z,i,p)_{type-agg}}} \cdot Q_{class_k} \end{aligned} \tag{3.2}$$

$$\begin{aligned} p_{(z,i,p)_{sector-agg}} &= \sum_l \%sector_l \cdot p_{k_{(z,i,p)_{class-agg}}} \\ q_{(z,i,p)_{sector-agg}} &= \frac{1}{Q_{total}} \sum_l \%sector_l \cdot q_{k_{(z,i,p)_{class-agg}}} \cdot Q_{sector_l} \end{aligned} \tag{3.3}$$

It is important to consider when doing the aggregation that the active power is being straight forward aggregated due to the energy conservation. But for the reactive power aggregation the contribution cannot be added directly, the power factor of each load must be taken into account [15].

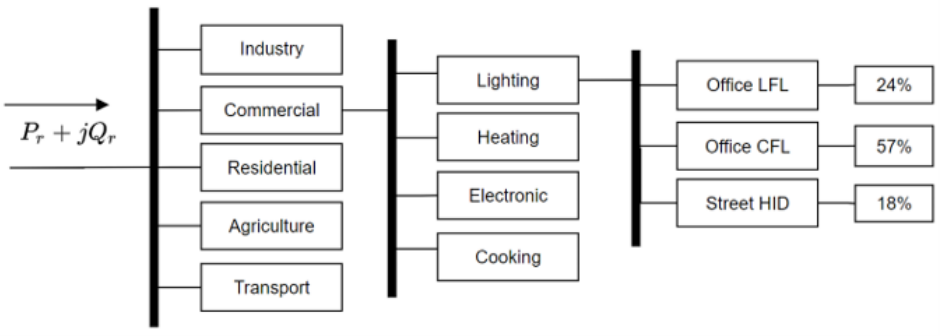

Figure 3.3: Aggregation Scheme - ZIP [15]

Induction Motors

The equivalent components in an induction motor are aggregated considering the energy conservation law [16]. There are several motors on each type, but the model will be represented with only one motor of each type.

$$
\begin{aligned}
R_{s_{agg}} &= \frac{\sum_{i=1}^{n} |I_{si}|^2 R_{si}}{\left|I_{s_{agg}}\right|^2} \\
R_{r_{agg}} &= \frac{\sum_{i=1}^{n} |I_{ri}|^2 R_{ri}}{\left|I_{r_{agg}}\right|^2} \\
X_{s_{agg}} &= \frac{\sum_{i=1}^{n} |I_{si}|^2 X_{si}}{\left|I_{s_{agg}}\right|^2} \\
X_{r_{agg}} &= \frac{\sum_{i=1}^{n} |I_{ri}|^2 X_{ri}}{\left|I_{r_{agg}}\right|^2} \\
X_{m_{agg}} &= \frac{\sum_{i=1}^{n} |I_{si} - I_{ri}|^2 X_{mi}}{\left|I_{s_{agg}} - I_{r_{agg}}\right|^2}
\end{aligned}
\tag{3.4}
$$

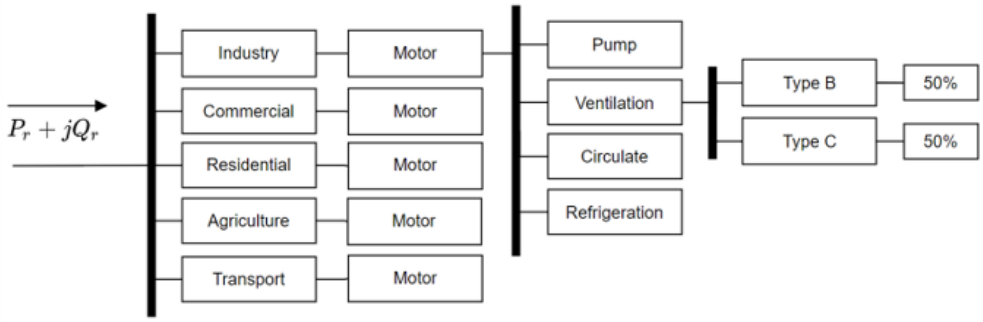

Figure 3.4: Aggregation Scheme - IM

To generalize, there are 3 types of motors (A, B and C) that will be considered in the grid. A big, medium, and small size with a power of 500, 75, and 0.75 horsepower, respectively.

To sum up, the load estimation approach method will be applied. When having all the loads that constitute the grid, with the use of the aggregating technique, a simplified composite model can be found.

Chapter 4

Development of the Composite Model

On this chapter, the steps used to build the equivalent model are presented. Starting from the electrical elements distribution (what type of loads can be found in an electrical system?), then going through their power estimated demand (for a small town, what is the estimated consumption of the motors, electronics, etc.?), and finalizing with the equivalent components aggregation (when having several motor type A, now it will be represented as a single type A motor with a higher power demand and with new electrical parameters), an approximate model can be constructed.

4.1 Composite Load Model

The Western Electricity Coordinating Council (WECC) has developed a model structure composed with 4 different types of motors, static loads, electronic loads, transformer, feeding line and shunt reactances [17]. Their main motivation was to have an model that represents the delayed voltage recovery behavior. They call it the Composite Load Model (CMPLD).

The idea of this model is to represent as close as possible the dynamic behavior of the existing grid. The main motivation for this work was based on the need to capture the realistic voltage fluctuation under perturbations for transient studies. Also, it is important to remark that this work focused many resources on the modeling of the Air conditioner Load (motor type D), due to the stalling effect in the voltage recovery process.

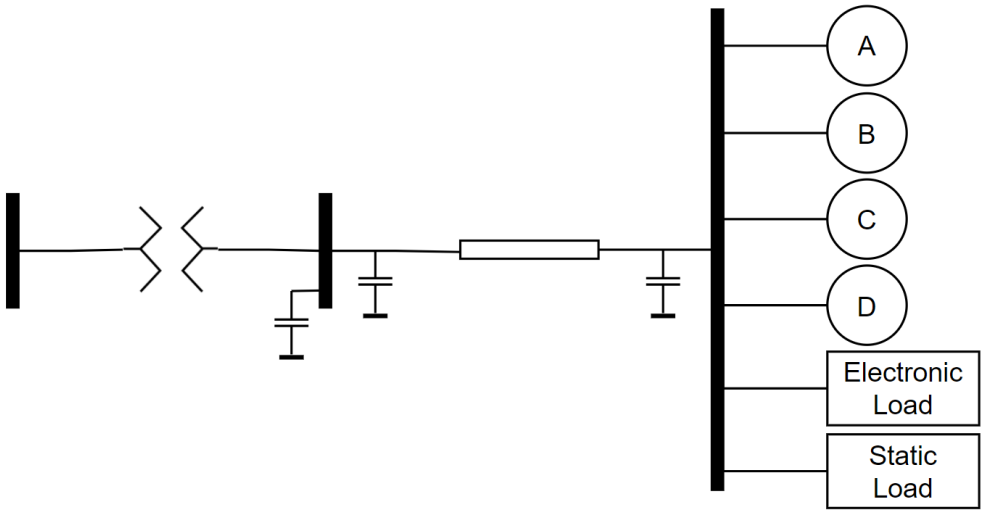

Figure 4.1: WECC Composite load model

This model considers large three-phase induction motors (A), medium three-phase IM (B), small three-phase IM (C), Air conditioner single-phase motor (D), electronic loads and static loads [18].

The software used for modeling and analysis is described in **section 1.2.1**. Respecting the limitations of this software, a single-phase load (unbalanced system analysis) can't be considered. This is why the Type D motor of the WECC model (see **figure 4.1**) is not taken into account.

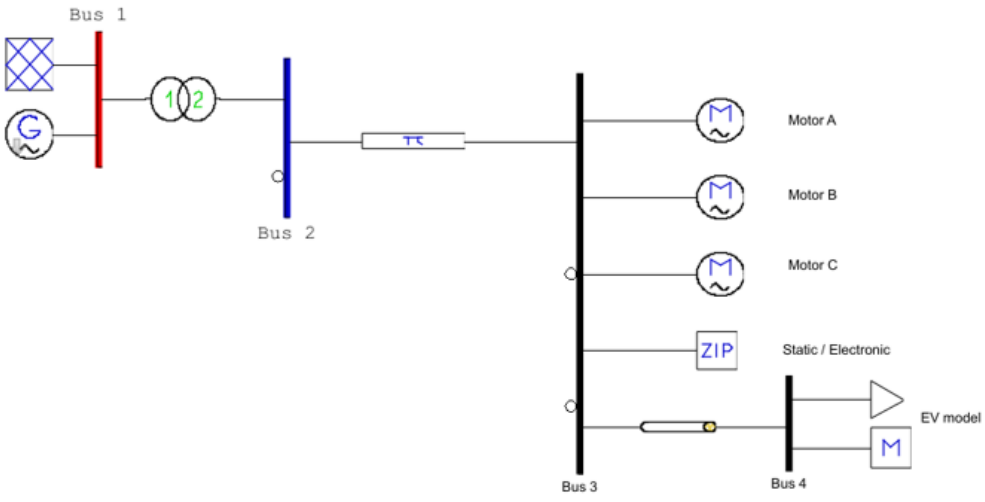

Figure 4.2: PSAT - Composite load model

The composite load model was built on a LV grid (400 V), with a transmission line ($Z_{line} = 0.001 + 0.02pu$, $B_{line} = 0.01$, electrical circuit in **figure 1.5**), and a MV/LV transformer ($Z_{transfomer} = 0.01 + 0.1pu$). Following the parameter aggregation discussed on **section 3.2.1**, the loads static and electronic are merged (aggregated). This mean, all the loads, other than motors and the electric vehicles type, will be represented by a single ZIP load (model explained in **section 2.2.1**).

Regarding the motors, each type (A, B or C) consists on the aggregation of the electric motors present in each of the sectors (as mentioned on **figure 3.2**). But these can be as well, merged into a single IM load for simplicity.

4.2 Model Development

The new load will consist approximately of a 10MW composite load. The power distribution through the different loads is indicated in the **appendix table C.1**.

4.2.1 Electronic and Static loads

Following the aggregation approach on [15], all the load types corresponding a ZIP equivalent can be merged together as explained in **section 3.2.1**. The different coefficients used for all the static and electronic equipment were found in [19].

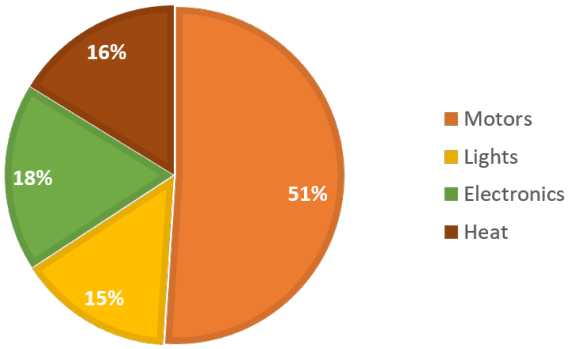

Figure 4.3: General Load Class

This figure represents an approximate class distribution of the load used for this project. The loads involving the lighting systems, the heating systems, and the electronics devices, are aggregated together. The final parameters for the ZIP type load is indicated on the **appendix table C.2**.

4.2.2 Induction Motors

To be able to quantify the motor load in the grid, according to the motor fraction of the total load (see **figure 4.3**), only the induction motor class was considered. Then from this point, 3 different sizes were included [20].

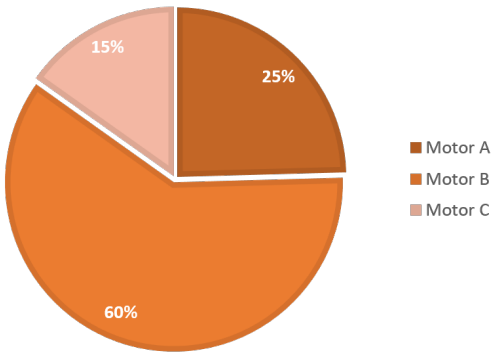

Figure 4.4: General distribution depending on IM type

As seen on **figure 4.3**, the IM is responsible for approximately half of the total electrical demand. The parameters used before the aggregation for each type of motor are indicated in **table 4.1**.

HP	**Rs[Ω]**	**Rr[Ω]**	**Xs[Ω]**	**Xr[Ω]**	**Xm[Ω]**	**J[kgm²]**	**H[kWs/kVA]**
500	0,012	0,035	0,041	0,040	2,099	8,500	0,344
75	0,420	0,140	0,150	0,150	9,470	0,980	0,265
0,75	4,860	1,840	2,670	2,670	84,680	0,005	0,128

Table 4.1: Single IM parameters

The quantity of motors aggregated for each of the types (A, B or C) were 3, 50 and 1259, respectively. For example, 3 motors of 500 hp are part of type A, which means that a total of 1500 hp make up this type.

Type	**HP_{agg}**	**Rs_{agg}[Ω]**	**Rr_{agg}[Ω]**	**Xs_{agg}[Ω]**	**Xr_{agg}[Ω]**	**Xm_{agg}[Ω]**
A	1500	0,0039	0,0117	0,0136	0,0135	0,6997
B	3750	0,0084	0,0028	0,0030	0,0030	0,1894
C	944	0,0039	0,0015	0,0021	0,0021	0,0673

Table 4.2: Aggregated IM parameters

To have a final simpler representation, depending on the fraction of power determined for each type of motor (see the **appendix table C.1**), the parameters are once more aggregated. The final parameters for the IM load is indicated on the **appendix table C.4**.

4.2.3 Electric Vehicles

Considering an increase in the electric vehicles in the following 20 years, it is protected to reach near a 10% of the electricity consumption in the grid [21]. This will now affect the previous load distribution (see **figures 4.3** and **3.2**), where this type of load was not contemplated.

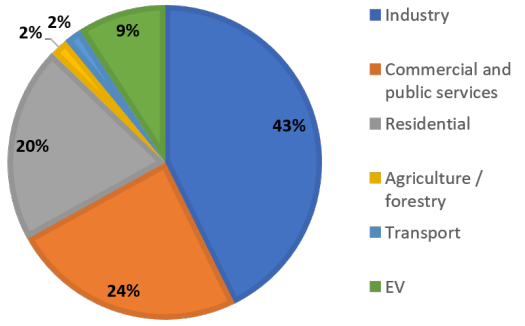

Figure 4.5: Consumption - Projection

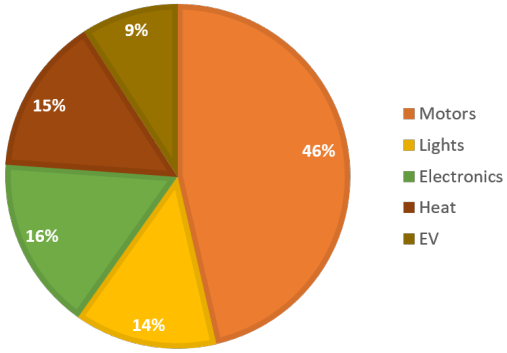

Figure 4.6: Load Class - Projection

Then considering a composite load of a total of 10MW, the fraction according to **figures 4.5** and **4.6** for the electric vehicle type load (EV) is represented in **table 4.3**.

$V[V]$	$P_1[kW]$	$Q_1[kVAr]$	$p.f.$	Qty	$P_{total}[kW]$	$Q_{total}[kVAr]$
400	10	2.9	0.96	91	910	265.4

Table 4.3: Residential EV charger load

Knowing that the model has a voltage dependent type load and a constant power type load (as seen in **equation 2.3**), it is needed to establish the power for each type of load taking into account the complete power of the EV charger load (see **table 4.3**). These values are represented in **table 4.4**.

a		b	
P [kW]	Q [kVAr]	P [kW]	Q [kVAr]
63.7	18.6	846.3	246.8

Table 4.4: EV Power Parameters

4.2.4 Residential Solar Panels

Around a 10% of houses in Belgium have solar panel to produce their own electricity. But this is just a small part of the complete system demand. It is important to remark that Belgium is committed to phase out the nuclear generation as part of their energy pact [7]. In the following years the use of renewable sources will significantly increase, specially for photovoltaic systems.

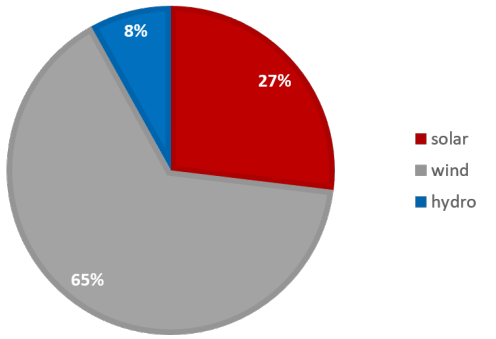

Figure 4.7: RES Belgium - 2019[14]

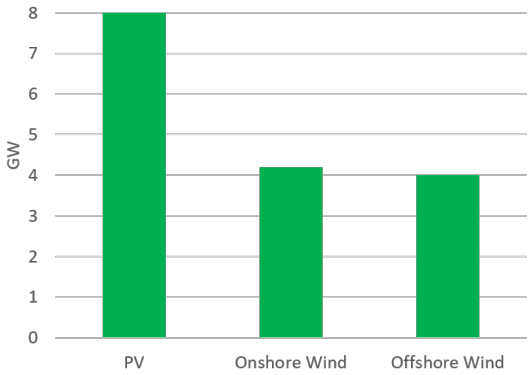

Figure 4.8: RES Belgium - 2030[7]

Although the data presented by ELIA [22], or by the IEA [14] are up to date, there is an issue regarding the PV generation which due to the lack of metering at low power/voltage systems, it is hard to measure the real generation in Belgium's houses.

Considering the study done in 2017 [23] strictly on residential prosumers, an estimation and a projection was made taking into account Wallonia and Flanders region. The estimation for the year 2019 can be seen in **figure 4.9**. The estimated average size of the installation for each of the residential solar PV (either on the Wallonia or Flanders region) is 3.87 kW.

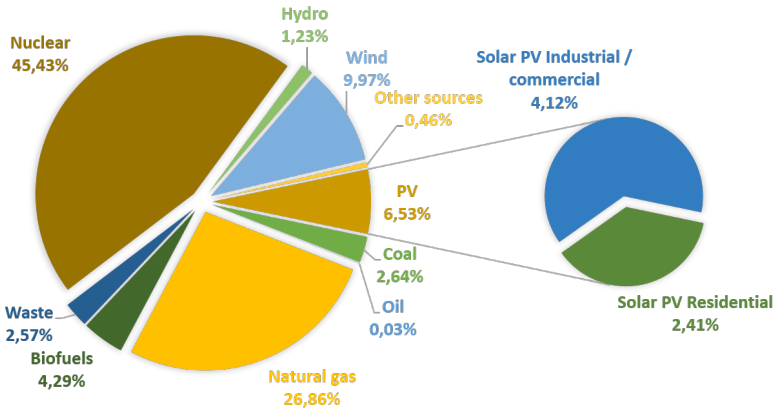

Figure 4.9: Electricity Generation by source 2019 - including residential PV

Now the model presented in **figure 4.2**, is updated including a distributed generation point for the residential PV equivalent in the grid.

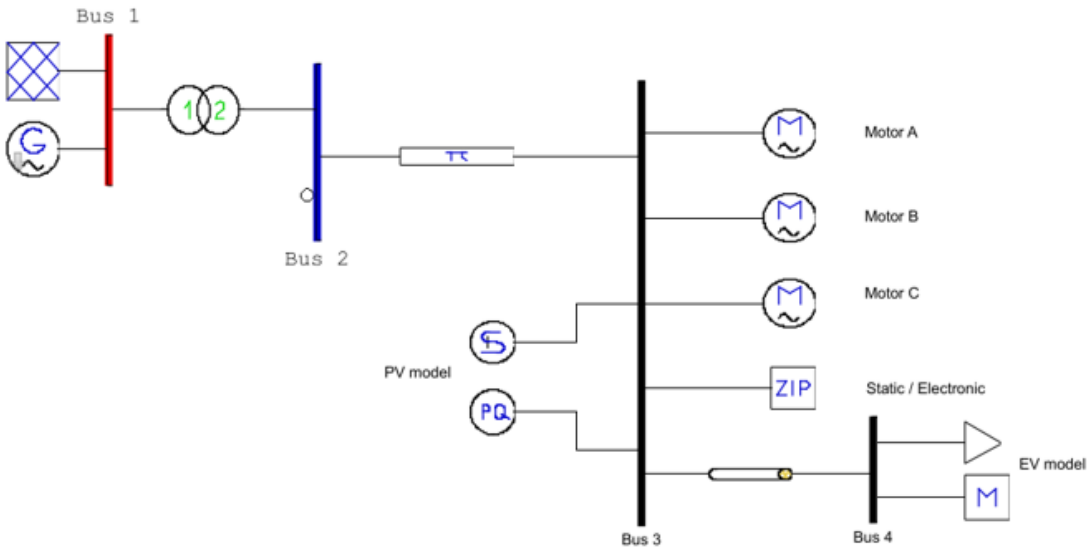

Figure 4.10: PSAT - CMPLD + DG

The power parameters used for the distributed generation source are indicated on the **appendix table C.1**. As considerations for the PV residential system, it does not help the grid to regulate a reference voltage. Although, it should include a constant monitoring mechanism that disconnect the DG when the voltage increases above the operational limit. In addition, the system is assumed to have a power factor of 0.99.

4.3 Model Behavior

This section will address the behavior of each type of load individually. The effect on the voltage stability of the overall system (combined loads) will also be analyzed.

4.3.1 ZIP

The ZIP model contains the aggregated values for the static and electronic loads (other than EV type) in the system. This model consists on the mixture of a constant impedance, a constant current, and a constant power type of load.

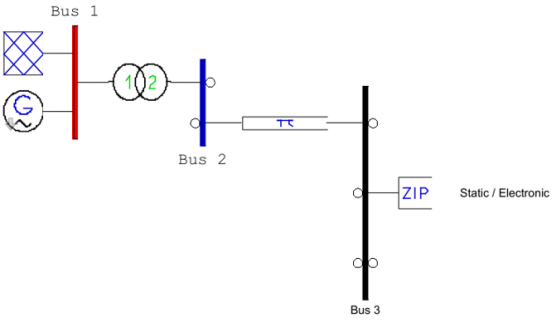

Figure 4.11: Only ZIP load - PSAT

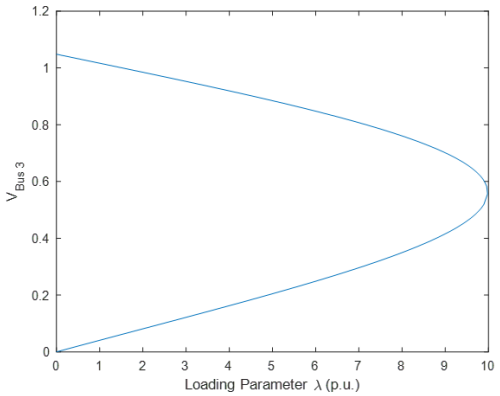

Figure 4.12: P-V curve for ZIP load

Once performed the voltage stability response on PSAT, the P-V curve method for the ZIP type of load is displayed on **figure 4.12**. It can be seen that this type of load is able to reach a loading parameter of approx. 10 (λ, it is a scalar variable that multiplies the load power demand).

4.3.2 IM

The IM model contains the values of the aggregated motors for each type as mentioned in **table 4.2**. The P-V curve method was done individually for each type of motor (A, B and C), and also with the aggregation of the 3 types.

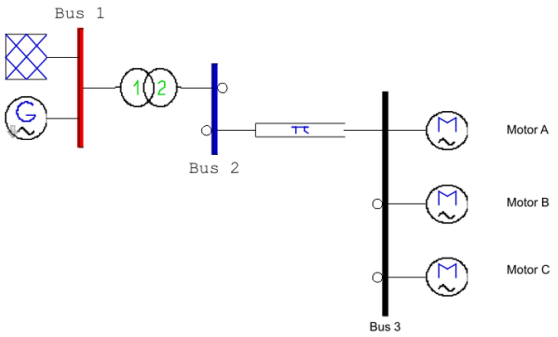

Figure 4.13: Only IM load - PSAT

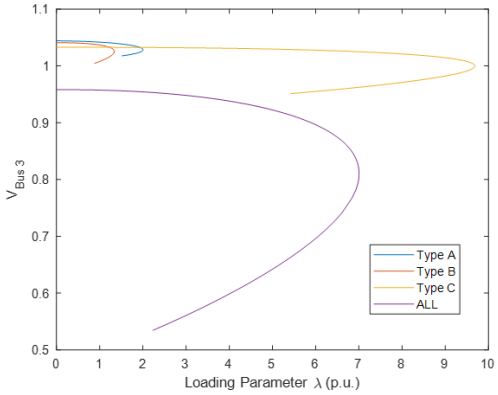

Figure 4.14: P-V curve for IM load

For a simpler approach, the complete aggregation into one single model is done. The P-V curve method for the single equivalent IM model is displayed on **figure 4.14**. The loading parameter reaches almost value 7 (λ), before entering in unstable region.

4.3.3 EV

The electric vehicle model is represented in PSAT with a static load and a voltage dependent load (as mentioned in **section 2.2.3,** sensitivity is linked to a negative exponent).

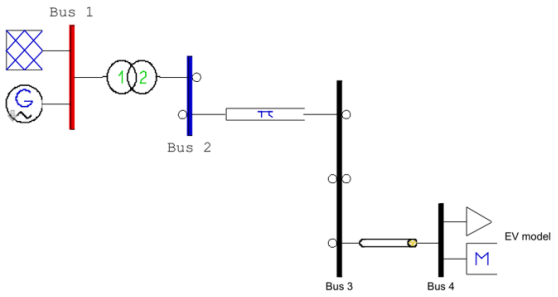

Figure 4.15: Only EV load - PSAT

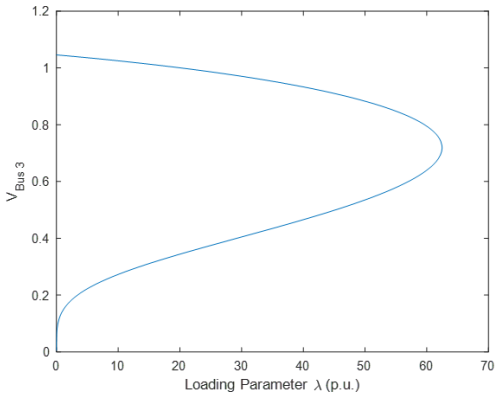

Figure 4.16: P-V curve for EV load

As mentioned in **figure 4.6**, the contribution of the EV type load is smaller in comparison either the ZIP (other static and electronics components on the grid) or the IM load. Therefore the loading parameter for only this type of load can reach such a high value.

4.3.4 CMPLD

With all the load types correctly defined, these contribute to the composite load model developed for this project (see **figure 4.17**).

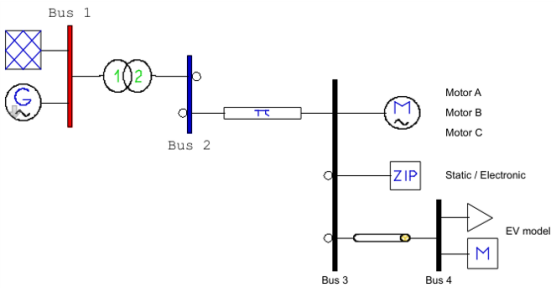

Figure 4.17: CMPLD load - PSAT

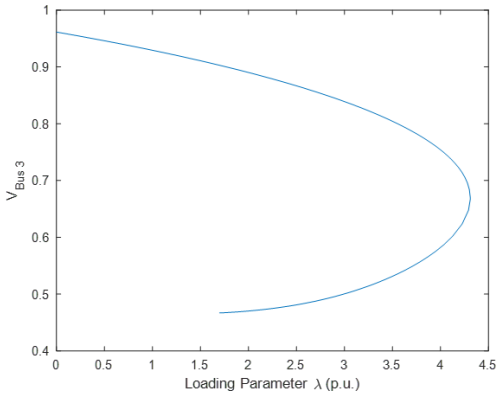

Figure 4.18: P-V curve for CMPLD load

It can be clearly seen that the new P-V curve considering all the loads has a lower loading parameter, shifting the nose (critical point) to the left. This means that the system can reach faster an instability state, or that it will be more sensible under any disturbance to fall into the unstable region.

4.3.5 CMPLD with DG

The composite load includes now a local generation caused by a residential photovoltaic distributed generation representation. This source has a main active power component due to the high-power factor used ($pf = 0.99$).

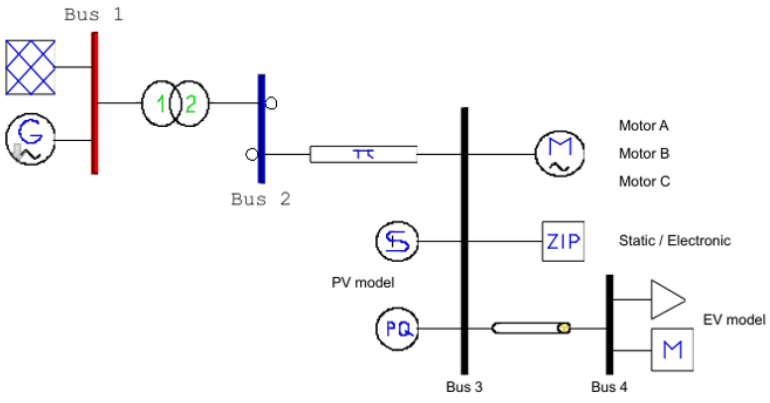

Figure 4.19: CMPLD load with Distributed Generation - PSAT

Although the value used for the distributed generation is small, several cases were simulated to analyze on PSAT the response of the voltage stability once the P-V method is applied.

Description		**kW**	**kVA**	**kVAr**
DG base case	2,4%	241	244	34
DG case 1	5%	500	505	71
DG case 2	10%	1000	1010	142
DG case 3	20%	2000	2020	285
DG case 4	50%	5000	5051	712
DG case 5	100%	10000	10101	1425

Table 4.5: Distributed Generation Cases

For the different cases, the base power is assumed to be 10 MW. Of course these are hypothetical assumption knowing that even considering the projection for 2030 done in [23], the residential PV could reach around 4-5% of the total electricity demand. For this scenario, for the Wallonia and Flanders region, the number of residential installations with solar PV will be near 15% (today, around a 10% of houses in Belgium have solar PV).

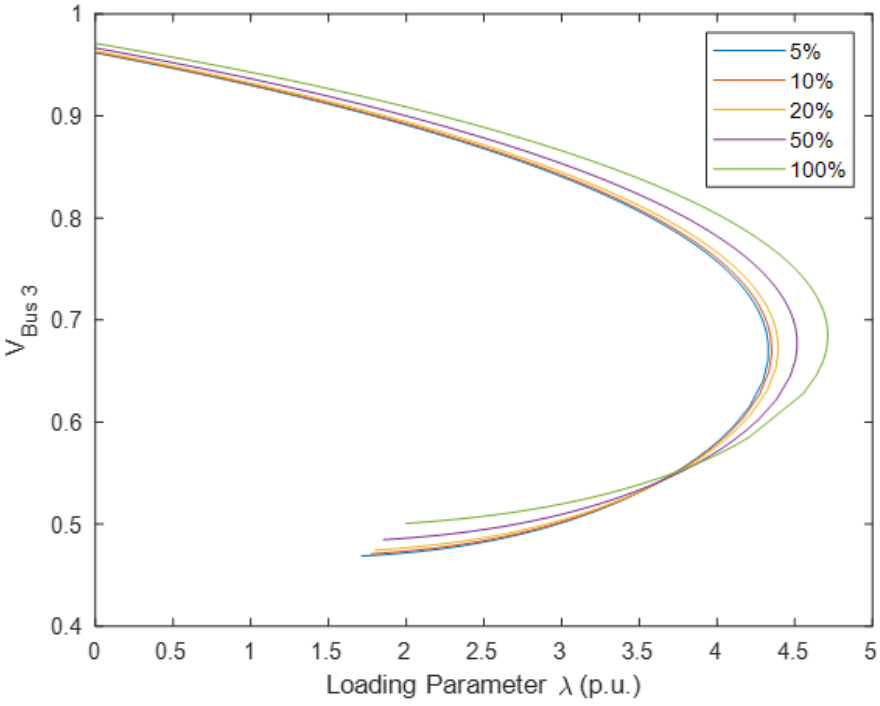

Figure 4.20: P-V curve for CMPLD load with Distributed Generation

Regarding the P-V curve of the system, the bigger the generation shifts the curve to the right allowing a bigger power variation before the nose is reached. It must be also taken into account the effect of the local generation on the voltage level in the system. The voltage profile in the low voltage grid has a higher level when the active power contribution increases.

To conclude this chapter, once done the respective simplifications and aggregations, the model that is used to represent a composite load is displayed in **figure 4.19**. This model is composed with an induction motor load type, a ZIP (polynomial) load type, an electric vehicle load type, and it includes a local distributed generation equivalent as well for a solar residential source.

Furthermore, it is important to mention that even in some areas the amount of PV has a much higher contribution in specific buses, not only 10% of the houses as mentioned in **section 4.2.4**. The contribution could increase up to 40% or even more (value obtained from personal visual perception).

Chapter 5

Study of the model developed on the IEEE 14 bus

On this last chapter, the model developed is tested on an IEEE bus. The process to have a valid simulation and analysis is carried out. Each step of the process is verified, and the pertinent corrections or adjustments are made when required by the system. This means that at nominal conditions, the base cased system with the new load type should be operating between acceptable limits on the grid.

5.1 System Setup

On this section, the values of the parameters will be set to perform a study according to valid operational conditions. Also, considerations regarding the system behavior and the deployment of the disturbances are presented.

5.1.1 Software Tool

Before starting using the model developed for this project, a quick validation was done using the same electrical grid model on 2 different software. This electric grid model consist on static loads, transmission lines, transformers and generators, distributed all over 9 buses (see **appendix figure A.1**). This model was developed by the Western System Coordinating Council (WSCC).

This was done to verify the results of a free (no warranty) tool such as PSAT[5] and an official professional tool such as PowerWorld[24], which also performs power flows analysis and voltage stability analysis with the P-V or the V-Q method.

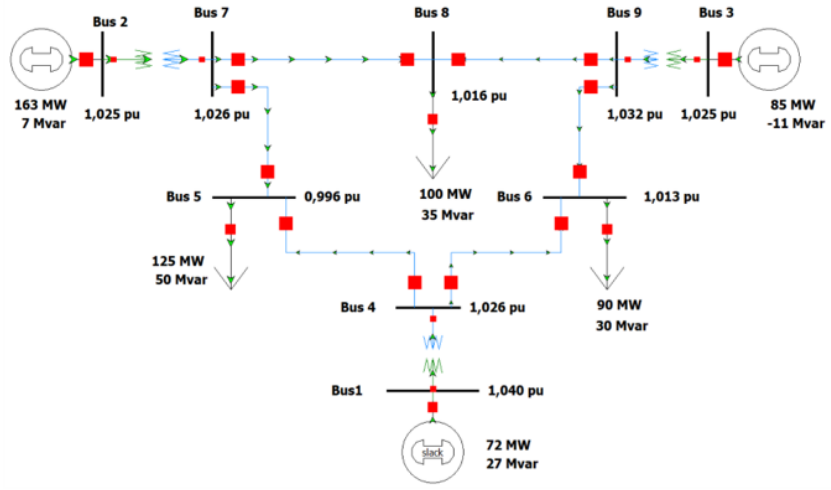

Figure 5.1: WSCC 9 bus test system - PowerWorld [5]

The first test was regarding the power flow in the system and the power profile on each of the buses. With this it was verified that the response on the 2 models is the same, the values corresponding the results on PSAT are displayed in the **appendix figures B.1, B.2, B.3** and **B.4**.

Now, the test will be related to the P-V curve of the system. For a simpler analysis, only the load in bus 5 will be considered, and as source, only the slack node (bus 1) will be considered.

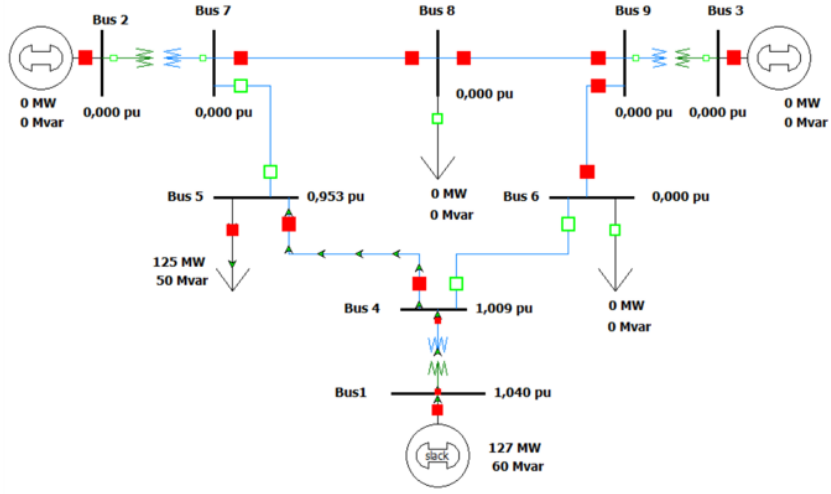

Figure 5.2: Single load/source - WSCC 9 bus - PowerWorld [5]

With this configuration, the P-V curve was be generated by increasing slowly the load until the critical point is reached. This type of bifurcation approach is known as the continuation power flow in PSAT (as briefly described in **section 1.2.1**).

The CPF method consist in obtaining the prediction step and the corrector step values, for finding the loading parameter (λ) that will be used for each power flow computation. The objective of each step is to reach the nose (critical point) for the system analyzed. The kind of bifurcation used to detect the voltage collapse behavior is the Saddle-node bifurcation (more information in [25]).

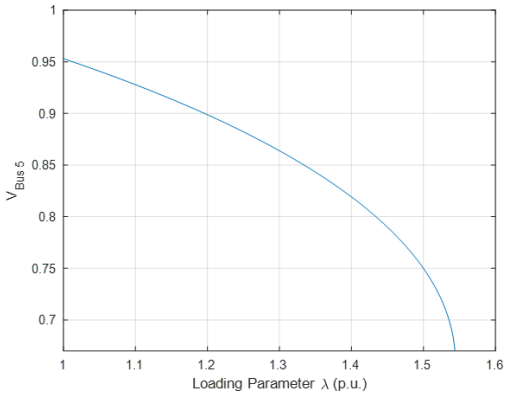

Figure 5.3: P-V WSCC PSAT

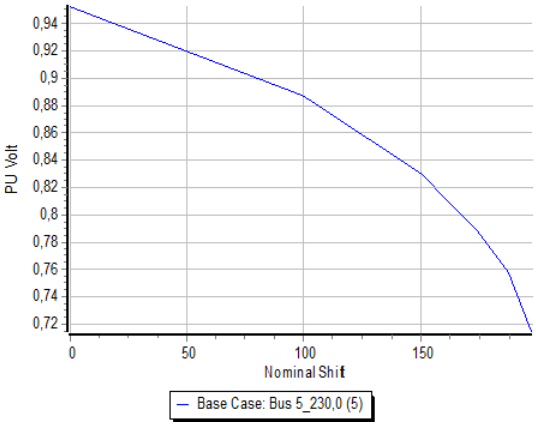

Figure 5.4: P-V WSCC PowerWorld

For both programs, the behavior of the curve and the critical point are quite similar. With this, the use of the free tool PSAT is validated, and it will be used on for further studies. Due to the limitations of the educational license for PowerWorld (max. 13 buses), this validation will no longer be done in this project.

5.1.2 Study Case

On this section, the final model that is used for stability voltage analysis is presented. Also, as part of the work, the guidelines were established to analyze the differences between using a static load model and using a composite load model in a predetermined grid model.

IEEE 14-Bus

The 14-bus model defined by the IEEE for research and test purposes was used. This electric grid model consist on static loads, capacitive compensators, transmission lines, transformers and generator, distributed all over 14 buses (see appendix figure [A.2]).

The base case results for the power flow computation on PSAT are displayed in the **appendix figures B.5, B.6, B.7** and **B.8**. For the base case, the response of voltage against the loading parameter (scalar variable that increases the load) is obtained.

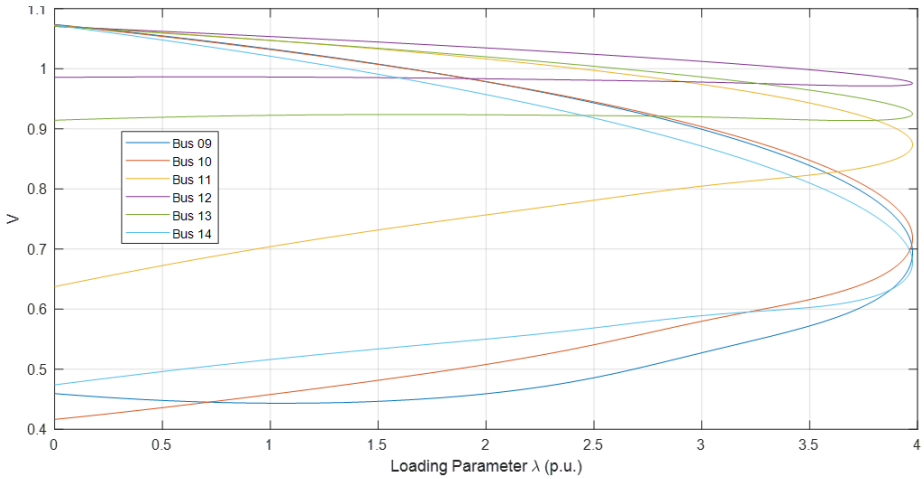

Figure 5.5: P-V curve - IEEE 14 bus - Base Case

The differences in shape are due to the different values of the equivalent impedance of the power feeding line to each system bus. The equivalent impedance of the load also influences the shape of the P-V curve. The general equivalent representation for the feeding line and the load can be seen in **figure 1.3**.

5.1.3 Additional considerations and verification of operating conditions

The model presented in **figure 4.10** will now be used inside the IEEE 14 bus model (see **appendix figure A.3**). For the study case, the composite model developed is placed on the bus 14. Being the most distant node located without any source connected, it is the most sensitive to disturbances. The power flow results (power profile and voltage profile) on PSAT are displayed in the **appendix figures B.9,**

B.10, B.11 and **B.12**.

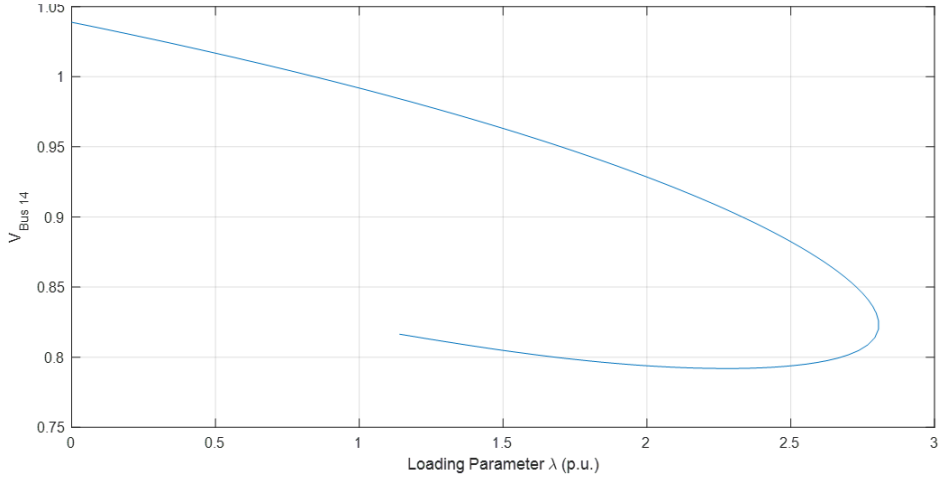

Figure 5.6: P-V curve - IEEE 14 bus with developed model

The P-V curve displays the system voltage stability response. The maximum loading parameter for the complete system is 2.8 (see **figure 5.6** for bus 14 and **figure 5.7** for bus 15). This means that the actual demanded load can increase x2.8 times before reaching the nose (critical point) leading to system collapse.

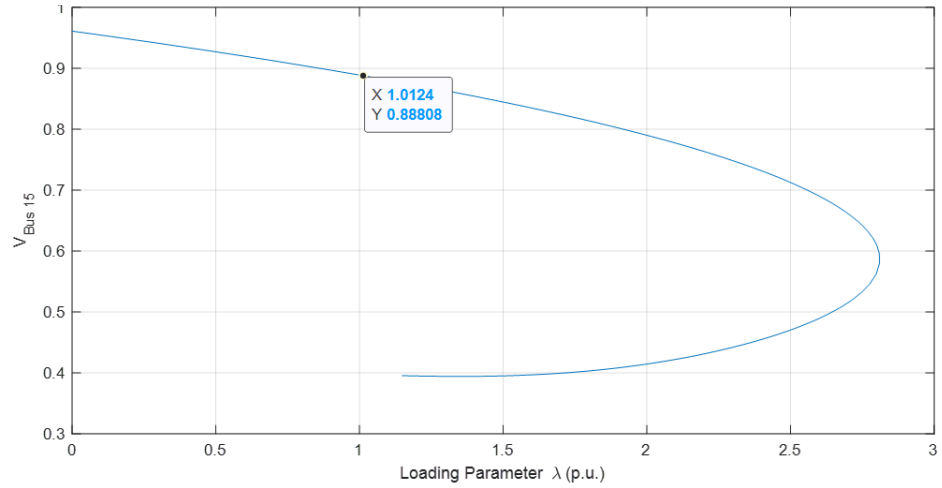

Figure 5.7: P-V curve - IEEE 14 bus - Voltage profile bus 15

Regarding the voltage levels on the power flow results (see the voltage magnitude on **appendix figure B.9**), it can be spotted that when the nominal load is

demanded ($\lambda = 1$), the voltage level of the bus 14 is below acceptable levels with a value of 0.88 pu. On the P-V curve method, this can be seen as well. This implies that at nominal conditions the system has a low voltage level, meaning that there must be something that should be done to increase the voltage profile. The voltage drop through the line connecting the bus 14 and the bus 15 is sufficiently high to affect the good operation of the system. The Critical limit for the voltage drop is 0.9 pu, below this value several low voltage devices will have problems.

5.1.4 Voltage Profile Correction

Two different methods were considered to improve the voltage profile in the low voltage bus. One involves a static reactive compensation on bus 15, and the other involves a tap setting in the MV/LV transformer connected on bus 14 (ideally an On-load tap-changer, OLTC).

Static Condenser

A static condenser compensation is installed on bus 15. Depending on the susceptance (or reactance) of the equivalent capacitor compensation system, the reactive power injected can be found.

$$\begin{aligned} Y &= \frac{1}{Z} = \frac{1}{R + jX} \\ Y &= G + jB \\ B &= 2\pi f C \\ Q &= V^2 B \end{aligned} \tag{5.1}$$

Being the susceptance (B [siemens]) the imaginary part of the admittance (Y [siemens]), some values of reactive power were used on the system to evaluate the response. On **table 5.1**, different cases were proposed.

#	V bus 15	B[pu]	MVAr
1	0,95	0,1	9,021
2	0,98	0,15	14,5
3	1,02	0,2	20,76
4	1,1	0,3	36,16
5	1,29	0,5	83,84

Table 5.1: Static Condenser Compensation

The new compensation parameters will have a direct effect on the voltage level of the bus where it is connected (bus 15). Using the smaller compensation (case 1) the system is able to go from an insufficient voltage level ($V = 0.88pu$, see **appendix figure B.9**) to a voltage value of 0.95 pu, which is adequate for a proper operation of the low voltage system. This will also help to improve the voltage level of neighboring buses.

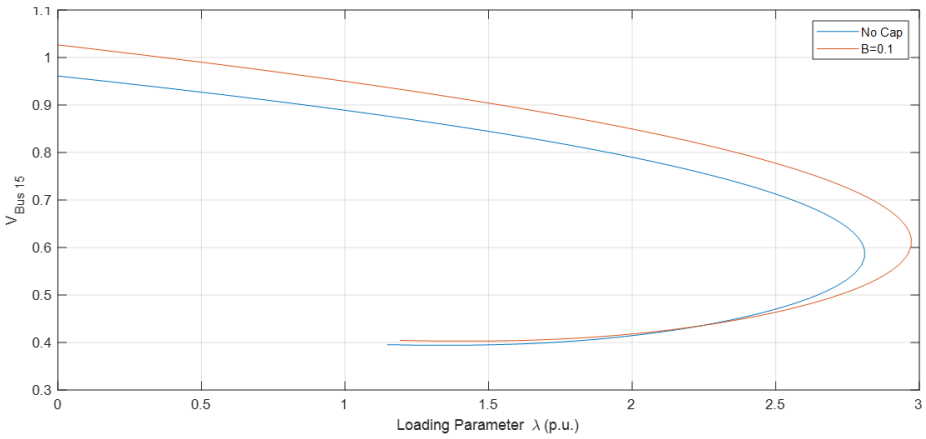

Figure 5.8: P-V curve - Voltage profile correction

It can be seen that the compensation improves the voltage profile for all the possible values of the load (variation of the loading parameter). For example, if we observe that the nominal load has increased 50% (loading parameter $\lambda = 1.5$ on **figure 5.8**), the voltage at bus 15 has increased from 0.84 to 0.9 pu with the reactive compensation.

It is important to remark that it will also affect the voltage stability of the system. If one node collapses, as mentioned before, the other buses will suffer instability as well (if control/protection mechanisms do not work in time). The P-V curve method for the different compensation cases is displayed in **figure 5.9**.

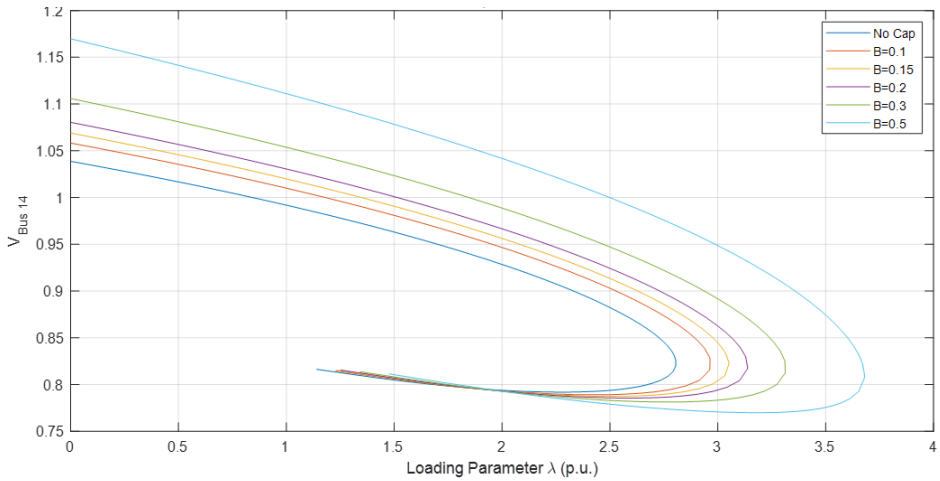

Figure 5.9: P-V curve - Different Compensation Values

Now regarding the stability, the curve is stretched to the right which means that the system is more robust to a power demand change.

Transformer Tap

On this case a two-winding transformer with tap change is considered. This transformer is modeled in PSAT as series reactances without iron losses. The different tap ratio cases are shown in **table 5.2**.

#	V bus 14	Tap Ratio	V bus 15
1	0,99	1	0,88
2	0,99	0,975	0,91
3	0,99	0,95	0,93
4	0,98	0,925	0,95

Table 5.2: Transformer Tap Change

This transformation parameters will have a direct effect on the voltage level of the secondary side (bus 15). Using the smaller tap value (case 4), the system is able to go from an insufficient voltage level ($V = 0.88pu$, see **appendix figure B.9**) to a voltage value of 0.95 pu, which is adequate for a proper operation of the low voltage grid. This will also help to improve the voltage level of neighboring buses.

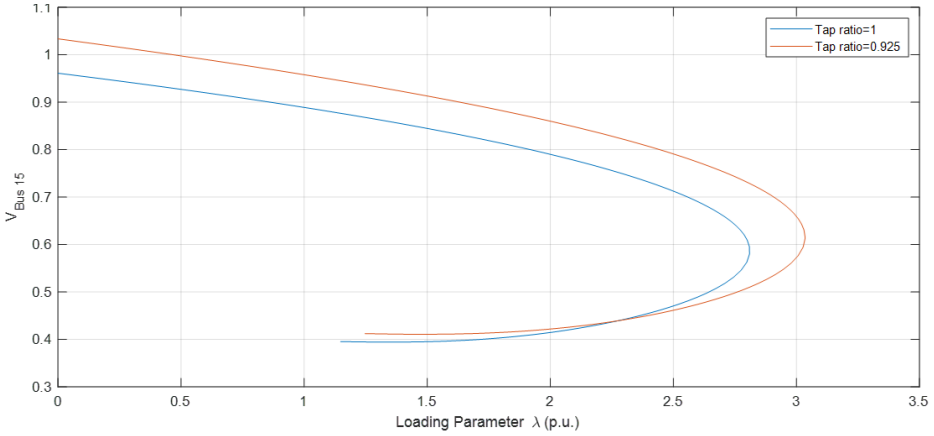

Figure 5.10: P-V curve - Voltage profile correction

Regarding voltage stability, the transformer tap change does not affect the voltage level at bus 14 but it allows the system to have a higher power demand before reaching instability. This can be seen in **figure 5.11**.

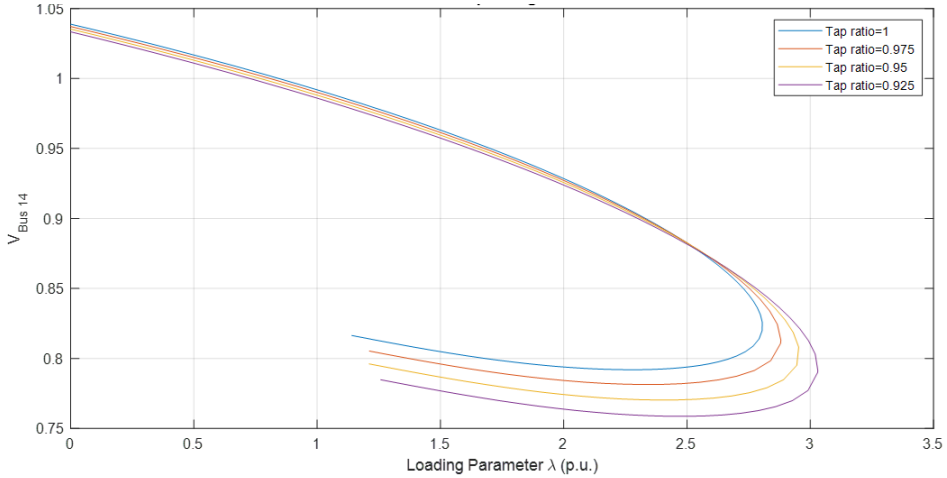

Figure 5.11: P-V curve - Different Tap Ratio Values

5.2 Contingencies

To check how the voltage stability of the system is affected, some perturbations are applied. The contingencies involve line loss, load loss or source (generation / compensation) loss.

#	Type	Location
1	Line loss	Bus 09 – Bus 14
2	Line loss	Bus 13 – Bus 14
3	Load loss	Bus 09
4	Load loss	Bus 04
5	Compensation loss	Bus 08
6	Source loss	Bus 02

Table 5.3: Perturbation Events

The analysis done, does not take into account the transient stability of the different perturbations. The fault (for example, a short circuit in a line) will not be analyzed in time domain. The element faulted is assumed to be taken out of service by the protection devices at a reasonable period of time, isolating or disconnecting the problem device from the grid without causing any harm to other electrical elements. This means that the system is assumed to be already in a steady state after the fault / disconnection (e.g., the line between bus 09 a bus 14 is no longer part of the system), and the voltage stability analysis applying the P-V curve method considers the complete system without this faulted / disconnected element.

5.3 Results and Discussion

On this last section the different results regarding the perturbations (see **table 5.3**) that were applied to the complete electrical system (see **appendix figure A.4**), will be presented. Also, the additional analysis, remarks and conclusions of the work will be provided.

5.3.1 Voltage Stability Results

Line loss

The first event contemplates a fault in the line connecting the buses 09 and 14. The second event contemplates a fault in the line connecting the buses 13 and 14. The P-V curve method for the voltage stability analysis of the events (1 and 2) at the bus 14 is shown in **figures 5.12** and **5.13**, respectively.

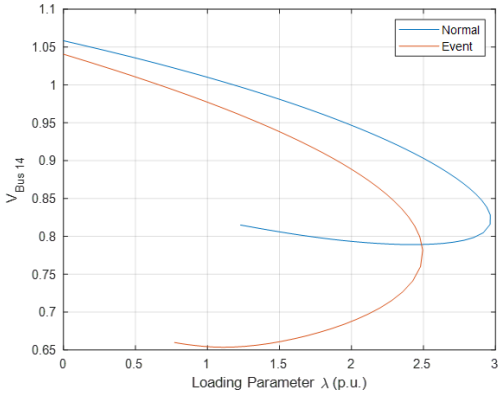

Figure 5.12: E_1 Loss:$Line_{Bus09-14}$

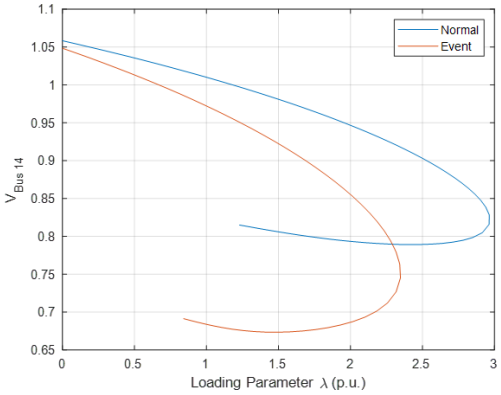

Figure 5.13: E_2 Loss:$Line_{Bus13-14}$

It is considered that the system correctly fulfils an N-1 contingency scenario. This means that it does not matter which of the lines is out of service, there is always a path to feed the load without breaching any of the operational limits that could affect the correct operation of the elements in the system (e.g. for the event 2, when there is no line between bus 13 and bus 14, the remaining operating line can support by itself the nominal power of the load at bus 14).

Load loss

The third event contemplates a fault in the load connected at the bus 09. The fourth event contemplates a fault in the load connected at the bus 04. The P-V curve method for the voltage stability analysis of the events (3 and 4) at the bus 14 is shown in **figures 5.14** and **5.15**, respectively.

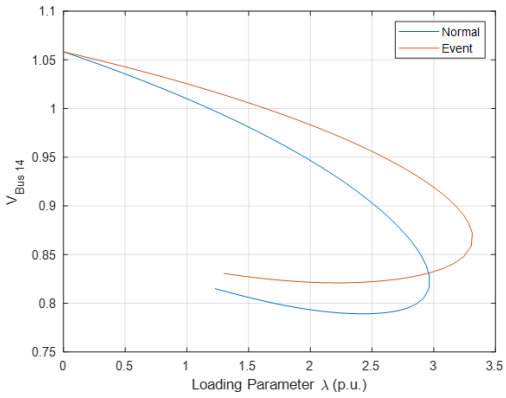

Figure 5.14: E_3 Loss:$Load_{Bus09}$

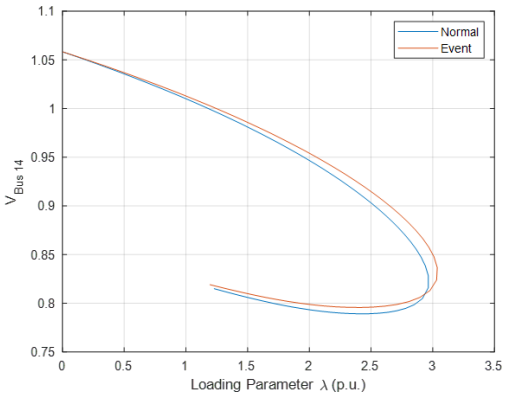

Figure 5.15: E_4 Loss:$Load_{Bus04}$

For the scenarios 3 and 4, a problem has occurred downwards the node of

connection (at bus 09 and 04, respectively). This led to the complete disconnection of the load. Now the equivalent impedance seen from the bus is infinite on the load side ($Z_{load} = \infty$).

Source loss

The fifth event contemplates a fault in the static synchronous compensation system connected at the bus 08. The sixth event contemplates a fault in the power generator connected at the bus 02. The P-V curve method for the voltage stability analysis of the events (5 and 6) at the bus 14 is shown in **figures 5.16** and **5.17**, respectively.

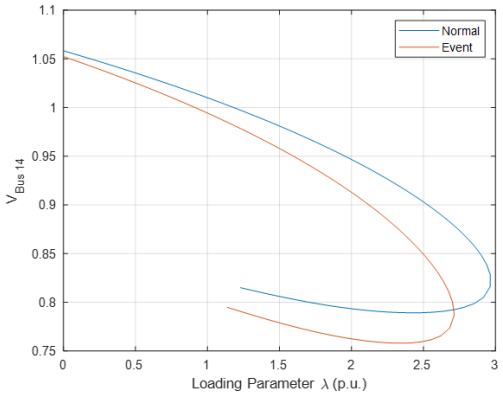

Figure 5.16: E_5 Loss:$STATCOM_{Bus08}$

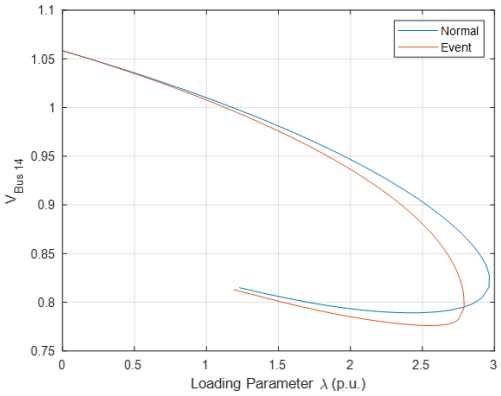

Figure 5.17: E_6 Loss:Gen_{Bus02}

Regarding the event 5, this lack of reactive compensation has a notorious effect on the voltage profile in the bus 14. For example, when the nominal load is operating, the voltage drops from 1.01 pu to 0.99 pu.

5.3.2 Conclusions and Analysis

On this project, it was presented the different responses of the system regarding the voltage stability analysis. There can be seen clearly the differences between the P-V curve obtained from the base IEEE 14 bus case (see **figure 5.5**), and the P-V curves for the model developed.

To be able to correctly analyze the voltage stability response in the grid, the system must be analyzed as a whole (not individual load types working). Considerable big loads have a significant influence on the network stability than others.

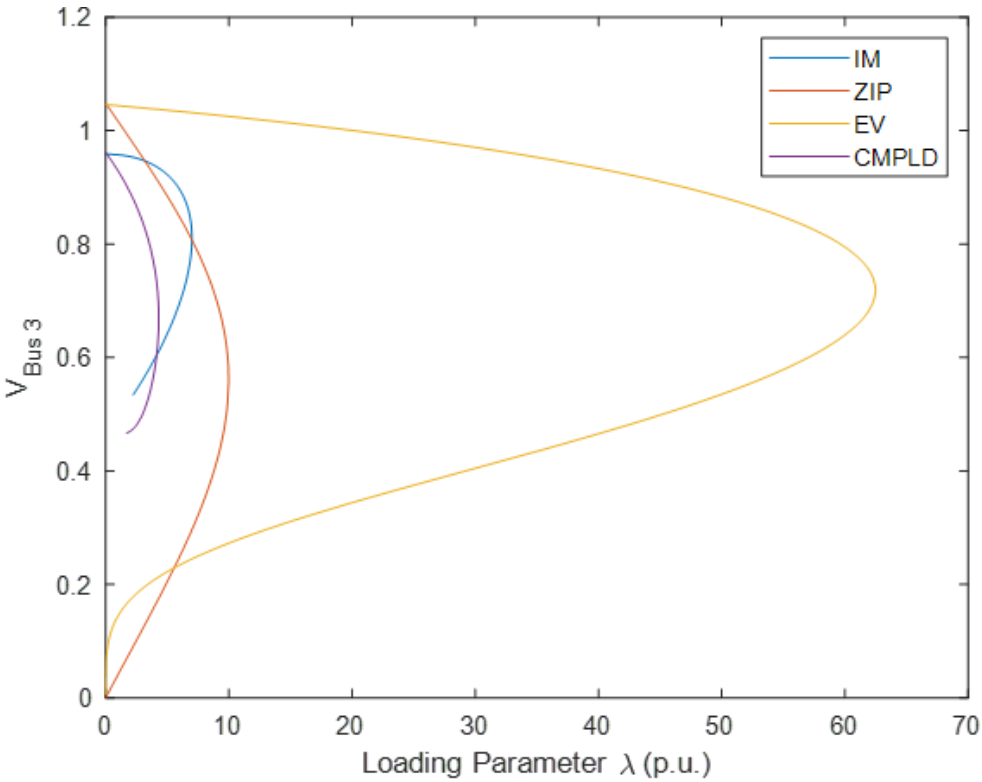

Figure 5.18: P-V curve for CMPLD load - Comparison

Each iteration of the power flow must consider the equivalent load representation from each node. The load is not analyzed individually, like presented in **figure 5.18**, but the equivalent electrical parallel elements will determine the system's voltage stability response.

Part of the scope of this project was to raise awareness on using the correct model to perform voltage stability analysis. For example, regarding the use of the CMPLD (see **appendix figures A.3** and **A.4**) the system has decrease the robustness. the system max power has decreased a 25%, before reaching a collapse stage. This is why this simplistic model should be used only for power flows studies (identify power transfer through electrical elements and voltage profile in the system buses), electrical equipment sizing (cables, transformers, etc.),

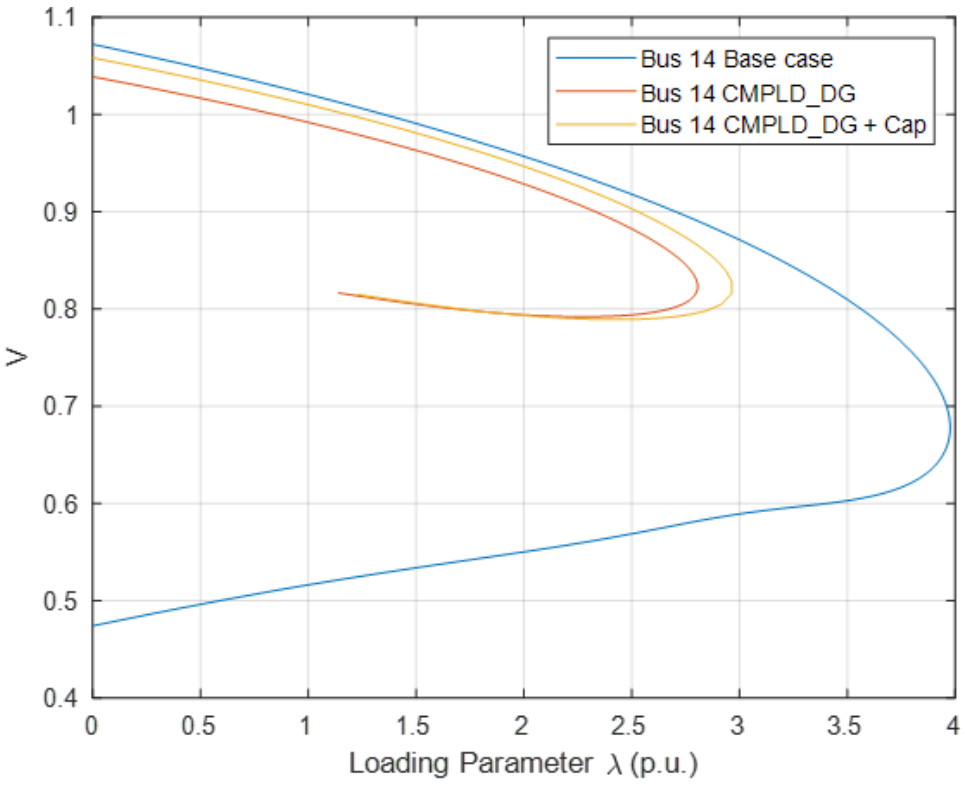

Figure 5.19: P-V curve for CMPLD with DG - Compensation

There can be spotted some general characteristics of the system from a voltage stability analysis, such as grid transmission power strength and reactive power limits of compensation. One of the purposes of the system operator is to supervise/monitor the system conditions to restrict the system from reaching a critical region (near the nose). The instability can be reached by various conditions [4] like the generation reactive capacity, the reactive compensation capability (e.g., synchronous compensator), the robustness of the transmission system and the load characteristics (power and composition). Additionally, the collapse conditions can be achieved if the control/protection strategies fail or are not correctly set.

It can be stated that among the possible contingencies that can occur in a transmission grid due to a system fault, from the ones that were contemplated on this work (see **figure 5.20**), the load disconnection events (3 and 4) were the only ones that had a positive effect regarding the voltage stability.

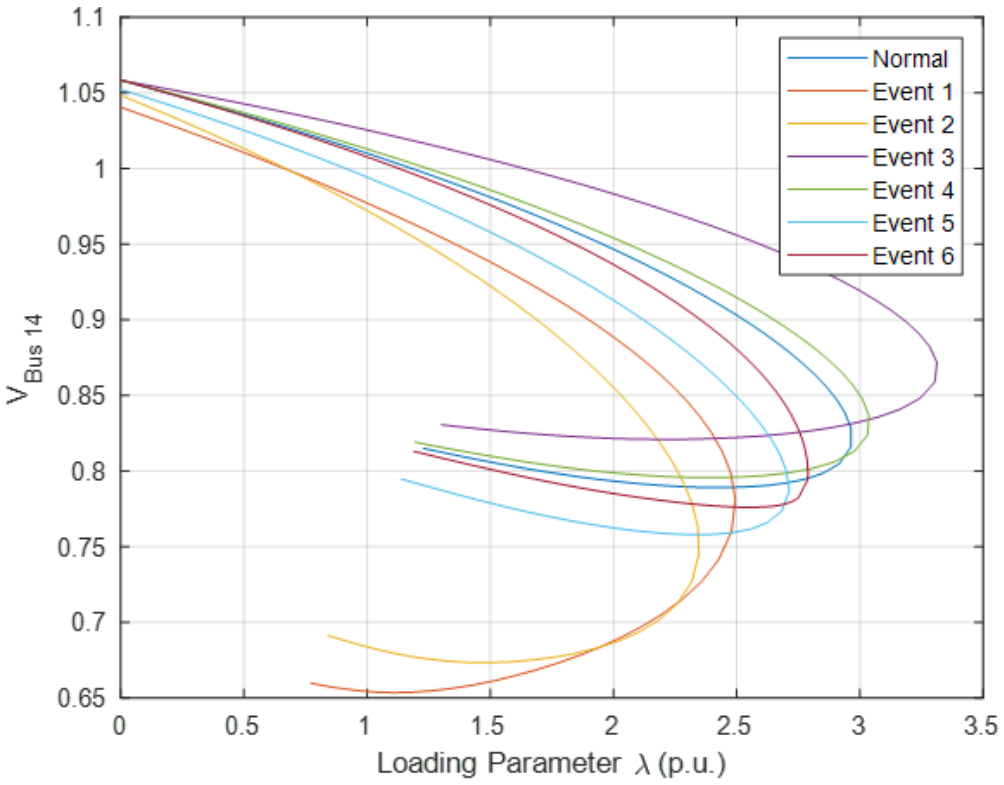

Figure 5.20: P-V curve for System Perturbations

All the other types of disturbances (event 1, 2, 5 and 6), decrease the strength of the grid limiting the power increase of the system. The worst cases (event 1 and 2) are when the circuit equivalent of the electrical feeding elements (impedance of the source + impedance of the transmission line) were drastically changed (e.g. line loss). This means that the load impedance change

When talking about power, the maximum power that can be transmitted over a transmission line is inversely proportional to its reactance (X_{line}). This is due to the Steady-State Stability Limit [4] obtained from $P_{max} = \frac{|V_S||V_R|}{X_{line}}$. Therefore, every time this impedance is affected (e.g., secondary/parallel line disconnection will increase the feeding impedance), the Steady-State Stability Limit decreases.

It is important to consider the voltage stability analysis for planning and operation purposes in the grid. When a new load wants to be included in the grid, the system operator must consider how increasing the load on a particular bus will affect the stability of the system. In addition, taking into account an electrical

load replacement, new technologies may have undesired behaviors in stability as well.

In operating conditions, if the system is correctly modeled, the operator can be aware of the real status of the system. This means that if the point of operation is not close to the bifurcation (critical point), there will not be needed to impose restrictions that will limit the power transfer in the grid.

In addition, voltage stability in principle is a local phenomenon. But when analyzing the consequences, it has a widespread impact that affects immediately adjacent buses. A way to avoid this is by monitoring constantly the conditions on the grid.

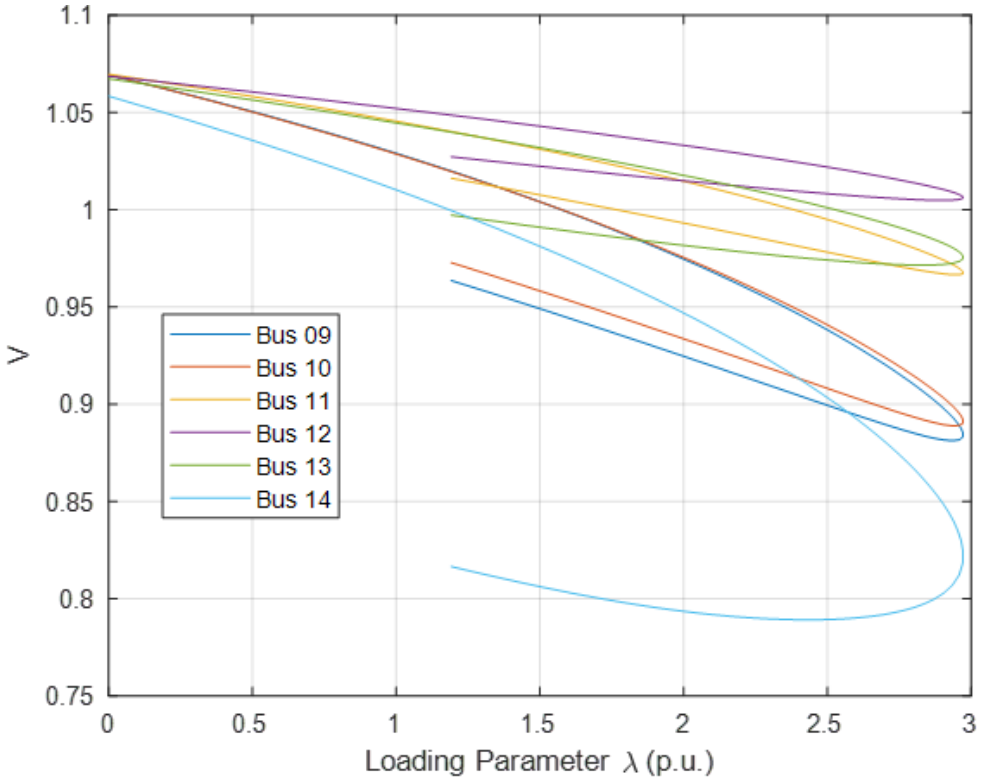

Figure 5.21: P-V curve for System Perturbations

This may mean that nearby nodes do not detect a drastic drop in voltage until it is too late, and they are already in the region of instability. Then, it is important to detect the stability problem locally to avoid a system collapse.

Regarding the solar distributed generation, it has a general good effect on the voltage stability performance (as seen on **figure 4.20**). But it is important to consider how the voltage profile is influenced by the power injection (which is mainly active power, pf>0.99). It increases the voltage level in the point (bus) of connection. But with the help of simple mechanisms of supervision and control, the solar PV system is disconnected to avoid any over-voltage. This disconnection effect can have a further problem on the system power management and stability, but this was not considered as part of the work.

To finalize, it is important to emphasize the important role that play System Operators regarding the operating conditions of the system. If they want to play safe and avoid being close to the bifurcation point (nose), they can impose several restrictions and constraints in the flow of power in the system. But having these limits can have economic negative effects and environmental issues, due to not being able to work at optimal operating points avoiding an efficient transfer of energy.

In conclusion, to ensure reliability and cost-efficient operations of the power system, it is crucial to have a realistic model. With this, voltage stability analyses can be carried out correctly, thus knowing how the system would respond to a maneuver, event, fault or even a future load growth (planning studies).

References

[1] M. S. S. Danish, T. Senjyu, S. M. S. Danish, N. R. Sabory, N. Krishnan, and P. Mandal, "A recap of voltage stability indices in the past three decades," *Energies*, vol. 12, p. 1544, Apr. 2019. DOI: 10.3390/en12081544.

[2] Y.-K. Wu, S. M. Chang, and Y.-L. Hu, "Literature review of power system blackouts," *Energy Procedia*, vol. 141, pp. 428–431, 2017, Power and Energy Systems Engineering, ISSN: 1876-6102. DOI: https://doi.org/10.1016/j.egypro.2017.11.055. [Online]. Available: https://www.sciencedirect.com/science/article/pii/S1876610217354619.

[3] S. Venkata, M. Eremia, and L. Toma, "Background of power system stability," in. Feb. 2013, pp. 453–475, ISBN: 9781118497173. DOI: 10.1002/9781118516072.ch8.

[4] T. Nagsarkar and M. Sukhija, *Power System Analysis SECOND EDITION*. Jan. 2014, ISBN: ISBN-10: 0-19-809633-X.

[5] F. Milano, "Matlab toolbox for static and dynamic analysis of electric power systems," *PSAT 2.1.11*, 2019. [Online]. Available: http://faraday1.ucd.ie/psat.html.

[6] NERC, "Technical reference document - dynamic load modeling," 2016. [Online]. Available: https://www.nerc.com/comm/PC/LoadModelingTaskForceDL/Dynamic%5C%20Load%5C%20Modeling020Tech%5C%20Ref%5C%202016-11-14%5C%20-%5C%20FINAL.PDF.

[7] A. JÄGER-WALDAU, "PV status report 2019 -European Commission," 2019. [Online]. Available: https://ec.europa.eu/jrc/sites/jrcsh/files/kjna29938enn_1.pdf.

[8] Y. Kongjeen and K. Bhumkittipich, "Modeling of electric vehicle loads for power flow analysis based on psat," in *2016 13th International Conference on Electrical Engineering/Electronics, Computer, Telecommunications and Information Technology (ECTI-CON)*, 2016, pp. 1–6. DOI: 10.1109/ECTICon.2016.7561430.

[9] C. Dharmakeerthi, N. Mithulananthan, and T. Saha, "Impact of electric vehicle fast charging on power system voltage stability," *International Journal of Electrical Power Energy Systems*, vol. 57, pp. 241–249, 2014, ISSN: 0142-0615. DOI: https://doi.org/10.1016/j.ijepes.2013.12.005. [Online]. Available: https://www.sciencedirect.com/science/article/pii/S0142061513005218.

[10] J. Lingyun, G. Chunlin, and Z. Fei, "The influence of induction motor on voltage stability of power system based on bifurcation theory," in *International Conference on Sustainable Power Generation and Supply (SUPERGEN 2012)*, 2012, pp. 1–6. DOI: 10.1049/cp.2012.1756.

[11] L. M. Vargas, J. Jatskevich, and J. R. Marti, "Induction motor loads and voltage stability assessment using pv curves," in *2009 IEEE Power Energy Society General Meeting*, 2009, pp. 1–7. DOI: 10.1109/PES.2009.5276032.

[12] H. Renmu, M. Jin, and D. Hill, "Composite load modeling via measurement approach," *IEEE Transactions on Power Systems*, vol. 21, no. 2, pp. 663–672, 2006. DOI: 10.1109/TPWRS.2006.873130.

[13] K. Yamashita, S. Djokic, J. Matevosyan, F. Resende, L. Korunovic, Z. Dong, and J. Milanovic, "Modelling and aggregation of loads in flexible power networks - scope and status of the work of cigre wg c4.605," *IFAC Proceedings Volumes*, vol. 45, no. 21, pp. 405–410, 2012, 8th Power Plant and Power System Control Symposium, ISSN: 1474-6670. DOI: https://doi.org/10.3182/20120902-4-FR-2032.00072. [Online]. Available: https://www.sciencedirect.com/science/article/pii/S1474667016320043.

[14] IEA, "Energy statistics data - belgium," 2021. [Online]. Available: https://www.iea.org/countries/belgium.

[15] A. P. Tellez, "Modelling aggregate loads in power systems," 2017. [Online]. Available: https://kth.diva-portal.org/smash/get/diva2:1085518/FULLTEXT01.pdf.

[16] P. Aree, "Aggregating method of induction motor group using energy conservation law," in *2013 10th International Conference on Electrical Engineering/Electronics, Computer, Telecommunications and Information Technology*, 2013, pp. 1–5. DOI: 10.1109/ECTICon.2013.6559506.

[17] Lawrence Berkeley National Laboratory, "Load modeling transmission researchs," *FINAL PROJECT REPORT*, 2010. [Online]. Available: https://web.eecs.umich.edu/~hiskens/publications/LM_Final_Report.pdf.

[18] A. Gaikwad, P. Markham, and P. Pourbeik, "Implementation of the WECC composite load model for utilities using the component-based modeling approach," in *2016 IEEE/PES Transmission and Distribution Conference and Exposition (T D)*, 2016, pp. 1–5. DOI: 10.1109/TDC.2016.7520081.

[19] A. Bokhari, A. Alkan, R. Dogan, M. Diaz-Aguiló, F. de León, D. Czarkowski, Z. Zabar, L. Birenbaum, A. Noel, and R. E. Uosef, "Experimental determination of the zip coefficients for modern residential, commercial, and industrial loads," *IEEE Transactions on Power Delivery*, vol. 29, no. 3, pp. 1372–1381, 2014. DOI: 10.1109/TPWRD.2013.2285096.

[20] P. Waide and C. U. Brunner, "Energy-efficiency policy opportunities for electric motor-driven systems," 2011. DOI: https://doi.org/https://doi.org/10.1787/5kgg52gb9gjd-en. [Online]. Available: https://www.oecd-ilibrary.org/content/paper/5kgg52gb9gjd-en.

[21] A. Klettke, A. Moser, T. Bossmann, P. Barberi, and L. Fournié, "Effect of electromobility on the power system and the integration of res," 2018. [Online]. Available: https://op.europa.eu/s/o0Y2.

[22] ELIA, "Solar-pv / wind - power generation data - belgium," 2021. [Online]. Available: https://www.elia.be/en/grid-data/power-generation.

[23] G. B. consortium, "Study on Residential Prosumers in the European Energy Union," 2017. [Online]. Available: https://ec.europa.eu/info/sites/default/files/study-residential-prosumers-energy-union_en.pdf.

[24] PowerWorld Corporation, "Powerworld simulator educational license," *Version 21*, 2020. [Online]. Available: https://www.powerworld.com/download-purchase/demo-software.

[25] Y. Ma, S. Lv, X. Zhou, Z. Gao, X. Zhang, and J. Zhang, "Analysis of voltage stability of power systems using the bifurcation theory," in *2018 Chinese Control And Decision Conference (CCDC)*, 2018, pp. 5150–5155. DOI: 10.1109/CCDC.2018.8408025.

Appendix A

Models

WSCC 9 Bus

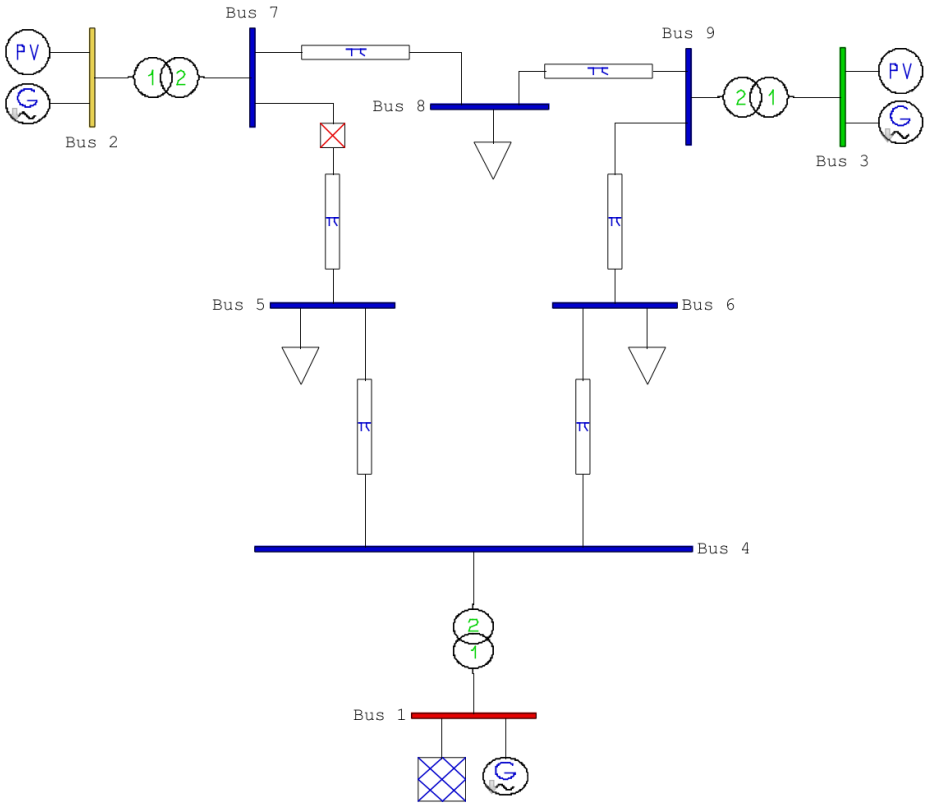

Figure A.1: WSCC 9 bus test system - PSAT [5]

IEEE 14 Bus

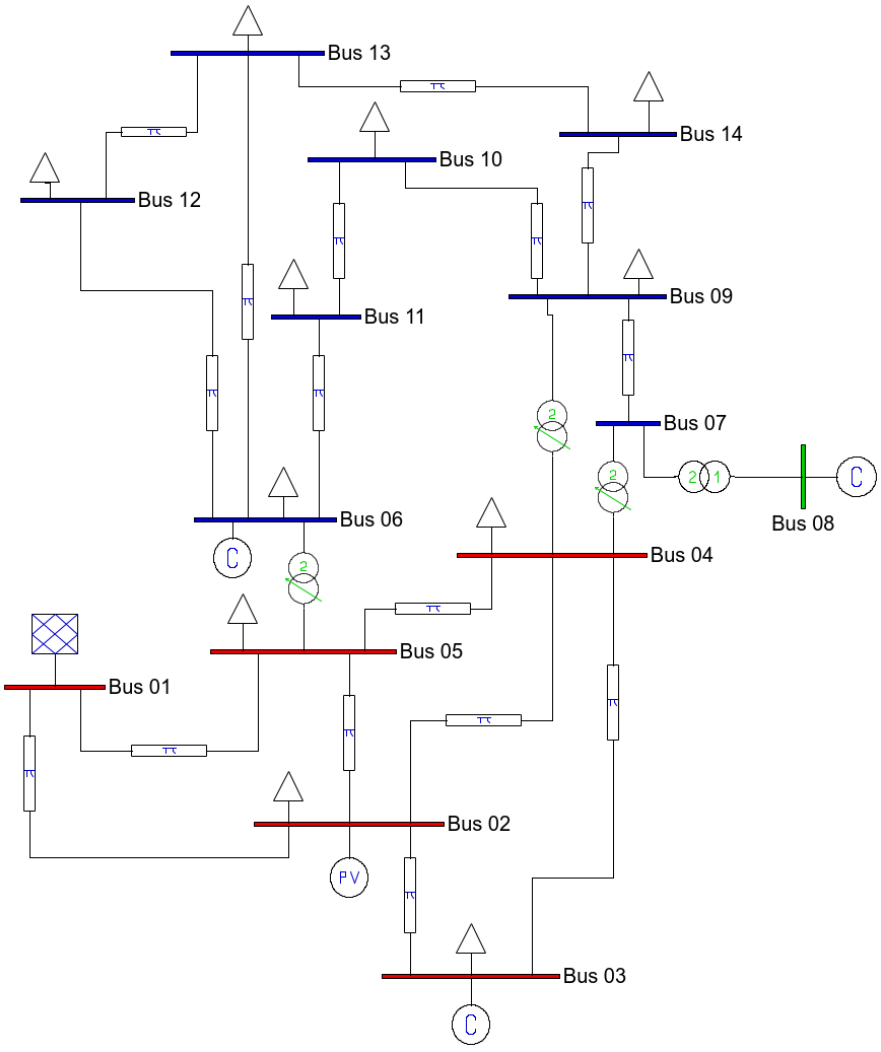

Figure A.2: IEEE 14 bus test system - PSAT [5]

IEEE 14 Bus with CMPLD model

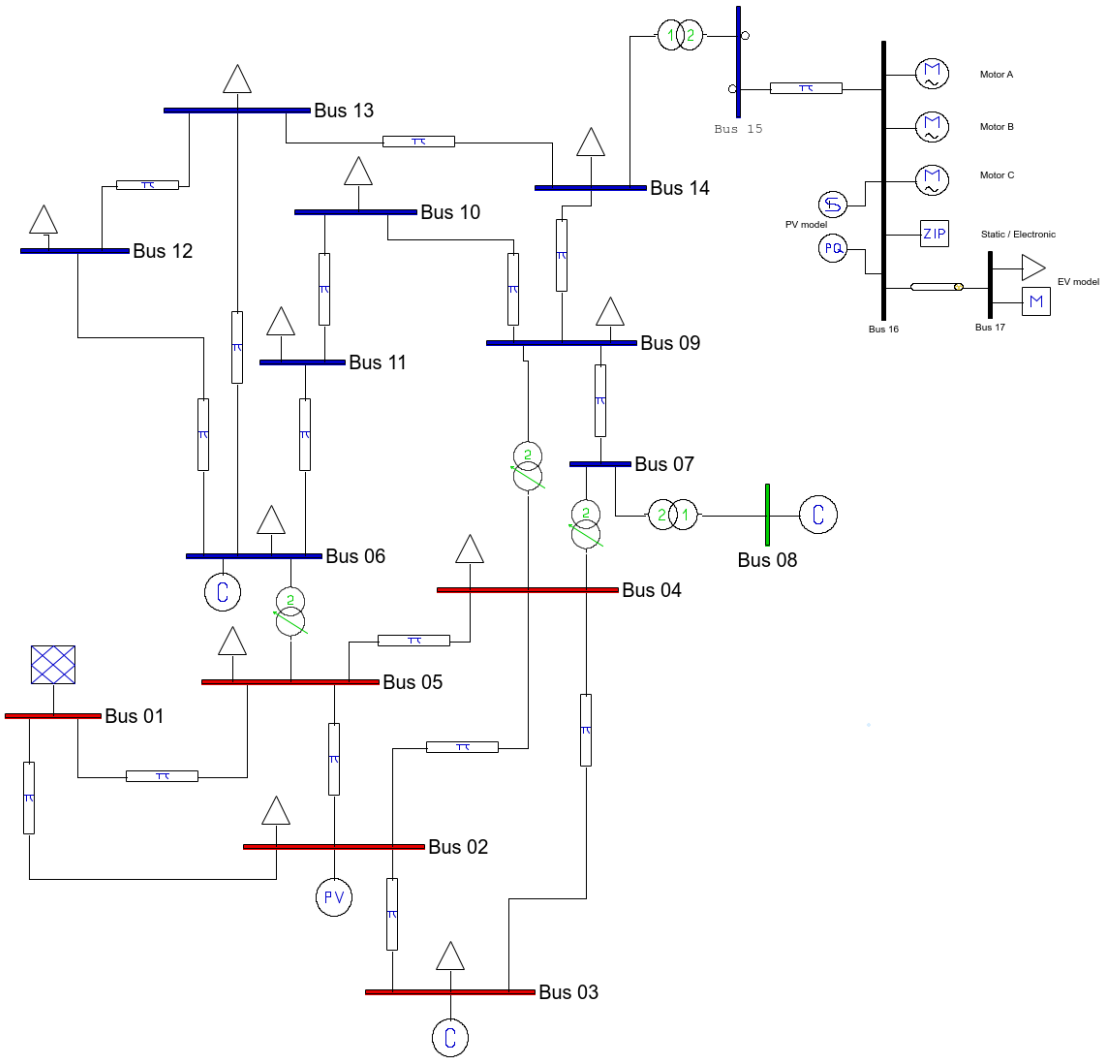

Figure A.3: IEEE 14 bus test system with model developed - PSAT [5]

IEEE 14 Bus with FINAL model

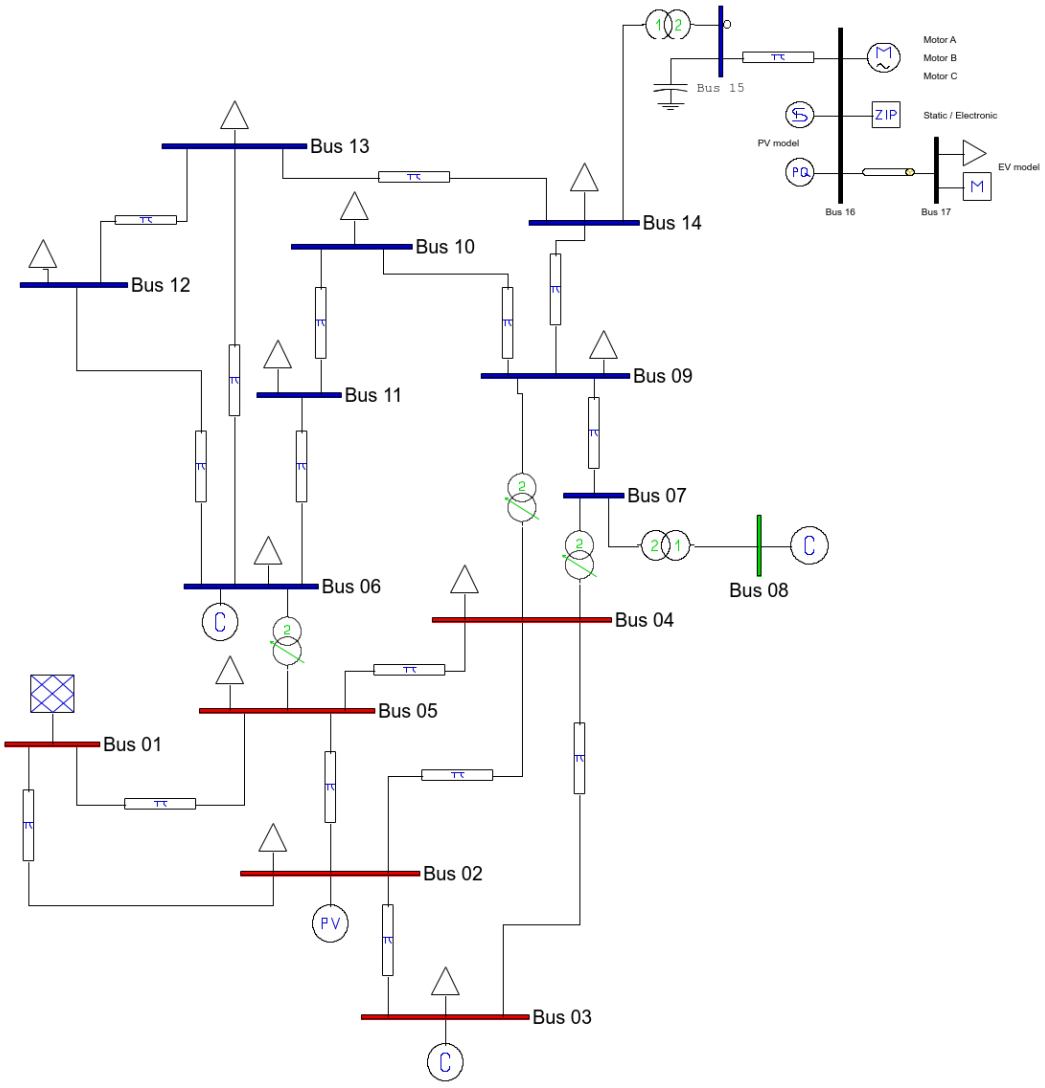

Figure A.4: IEEE 14 bus test system with FINAL model - PSAT [5]

Appendix B

Power Flow Results

WSCC 9 Bus

The following figures correspond to the power flow results on the general case for the model represented in figure [A.1].

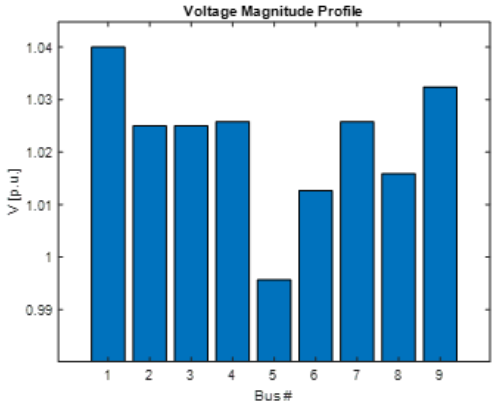

Figure B.1: Voltage magnitude

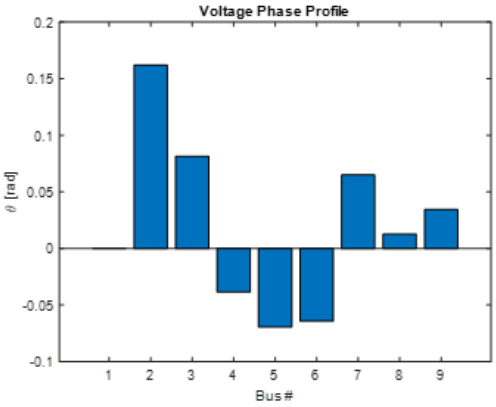

Figure B.2: Voltage angle

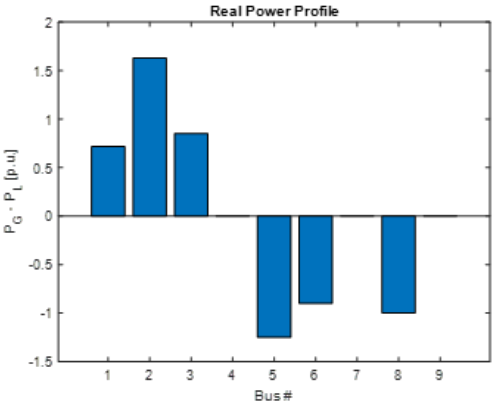

Figure B.3: Active power

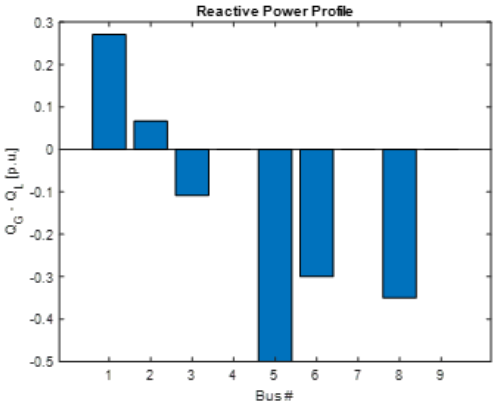

Figure B.4: Reactive power

IEEE 14 Bus

The following figures correspond to the power flow results on the general case for the model represented in figure [A.2].

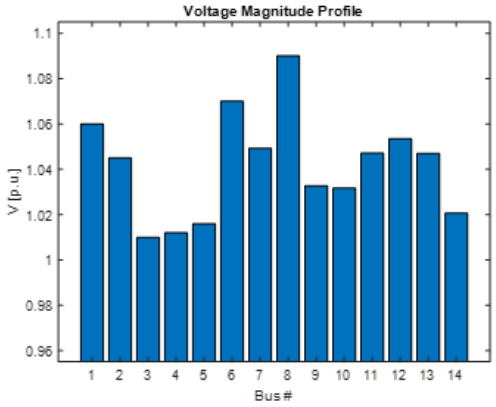

Figure B.5: Voltage magnitude

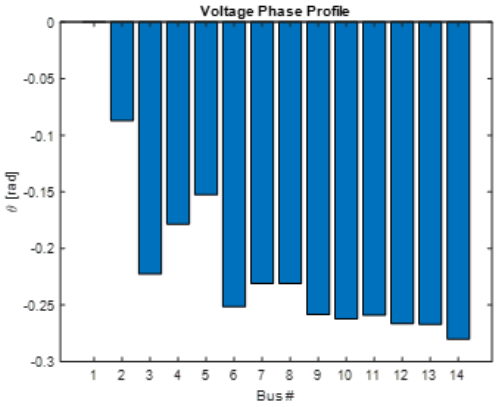

Figure B.6: Voltage angle

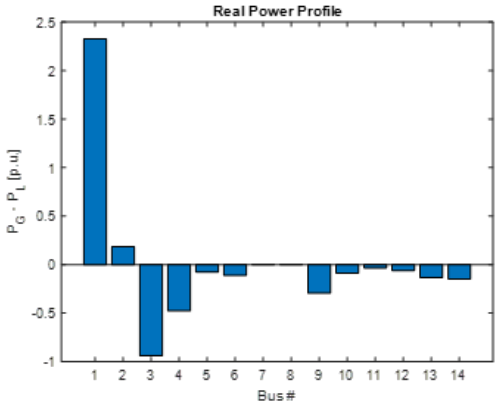

Figure B.7: Active power

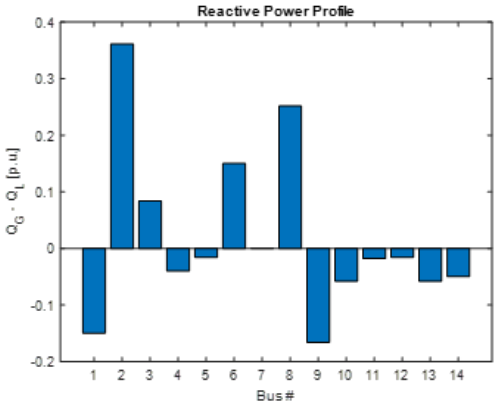

Figure B.8: Reactive power

IEEE 14 Bus with model CMPLD

The following figures correspond to the power flow results on the general case for the model represented in figure [A.3].

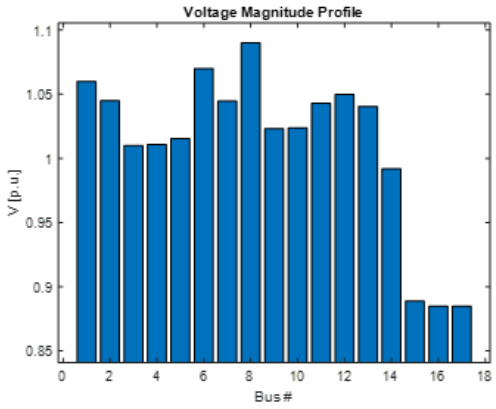

Figure B.9: Voltage magnitude

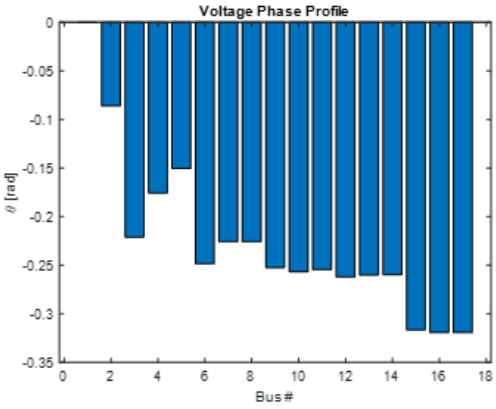

Figure B.10: Voltage angle

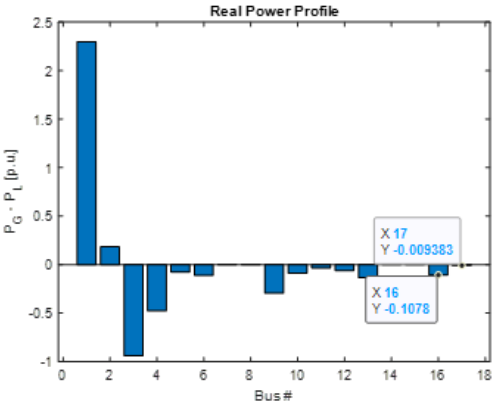

Figure B.11: Active power

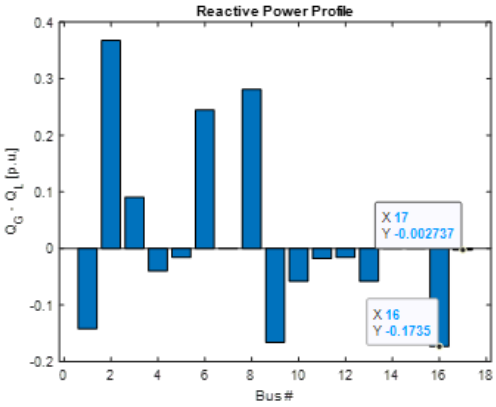

Figure B.12: Reactive power

IEEE 14 Bus with FINAL model

The following figures correspond to the power flow results on the general case for the FINAL model developed, represented in figure [A.4].

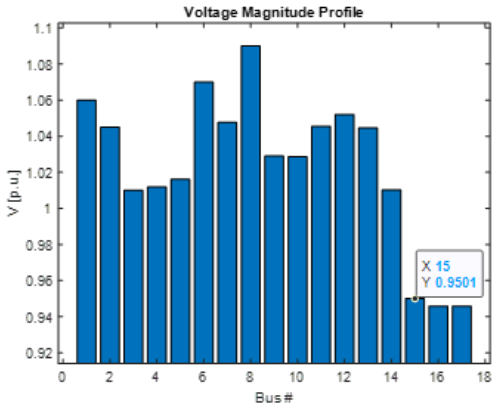

Figure B.13: Voltage magnitude

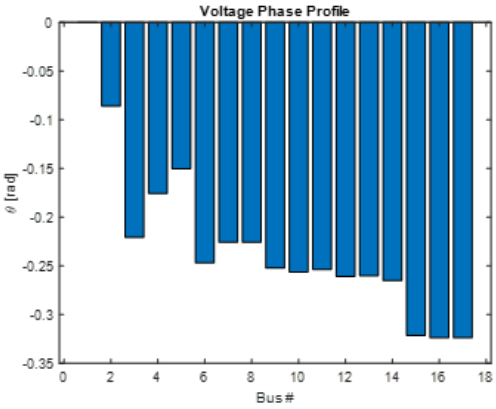

Figure B.14: Voltage angle

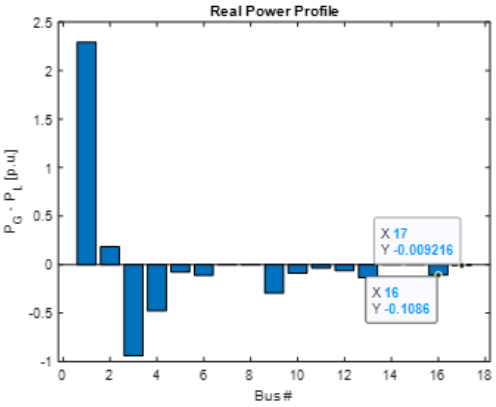

Figure B.15: Active power

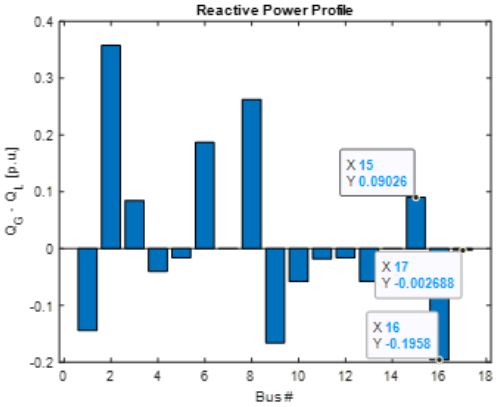

Figure B.16: Reactive power

Appendix C

Model Parameters

Description		kWh	Aggregate				Total		
			hp	kW	kVA	#	kW	kVAr	kVA
Motor A	46%	1140	500	373	439	3	1119	693	1316
Motor B		2795	75	56	66	50	2796	1733	3290
Motor C		704	0,75	0,56	0,66	1259	704	436	828
ZIP	45%	4452	-	4452	4917	1	4452	2087	4917
EV	9%	909	-	10	10	91	910	265	948
DG (source)	2,4%	241	-	-	-	-	241	34	244

Table C.1: Power parameters

Zp	Ip	Pp	Zq	Iq	Pq	pf
0,164	0,054	0,781	1,643	-1,917	1,274	0,905

Table C.2: ZIP parameters

Single				Total			a (exp)		b (constant)	
V	pf	kW	kVAr	Qty	kW	kVAr	kW	kVAr	kW	kVAr
400	0,96	10	2,92	91	910,00	265,42	63,70	18,58	846,30	246,84

Table C.3: EV parameters

Power_agg	Rs_agg	Rr_agg	Xs_agg	Xr_agg	Xm_agg	H_agg
MVA	Ω	Ω	Ω	Ω	Ω	kWs/kVA
5,43E+00	4,61E-04	1,84E-04	2,56E-04	2,55E-04	8,97E-03	2,63E-01

Table C.4: IM parameters

UNIVERSITÉ CATHOLIQUE DE LOUVAIN
École polytechnique de Louvain
Rue Archimède, 1 bte L6.11.01, 1348 Louvain-la-Neuve, Belgique | **www.uclouvain.be/epl**